

1 **Quantification of Terrestrial Ecosystem Carbon Dynamics in the Conterminous United States**

2 **Combining a Process-Based Biogeochemical Model and MODIS and AmeriFlux data**

3 Min Chen^a, Qianlai Zhuang^{a,b}, David R. Cook^c, Richard Coulter^c, Mikhail Pekour^d, Russell L. Scott^e, J.

4 William Munger^f, Ken Bible^g

5
6 ^aDepartment of Earth & Atmospheric Sciences, Purdue University, West Lafayette, IN, USA

7 ^bDepartment of Agronomy, Purdue University, West Lafayette, IN, USA

8 ^cClimate Research Section, Environmental Science Division, Argonne National Laboratory, Argonne,
9 IL, USA

10 ^dAtmospheric Sciences and Global Change Division, Pacific Northwest National Laboratory, Richland,
11 WA, USA

12 ^eSouthwest Watershed Research Center, USDA-ARS, Tucson, AZ, USA

13 ^fDivision of Engineering and Applied Sciences and Department of Earth and Planetary Sciences,
14 Harvard University, Cambridge, MA, USA

15 ^gWind River Canopy Crane Research Facility, University of Washington, WA, USA

16
17 Corresponding author: Min, Chen. Addresses: CIVIL Engineering Building, 550 Stadium Mall Drive,
18 West Lafayette, IN, 47907-2051, United States. Email: chenm@purdue.edu

19 Running Title: Quantification of Terrestrial Ecosystem Dynamics in the Conterminous U.S.

20 (Submitted to *Biogeosciences*)

21 **Abstract**

22 Satellite remote sensing provides continuous temporal and spatial information of terrestrial
23 ecosystems. Using these remote sensing data and eddy flux measurements and biogeochemical models,
24 such as the Terrestrial Ecosystem Model (TEM), should provide a more adequate quantification of
25 carbon dynamics of terrestrial ecosystems. Here we use Moderate Resolution Imaging
26 Spectroradiometer (MODIS) Enhanced Vegetation Index (EVI), Land Surface Water Index (LSWI) and
27 carbon flux data of AmeriFlux to conduct such a study. We first modify the gross primary production
28 (GPP) modeling in TEM by incorporating EVI and LSWI to account for the effects of the changes of
29 canopy photosynthetic capacity, phenology and water stress. Second, we parameterize and verify the
30 new version of TEM with eddy flux data. We then apply the model to the conterminous United States
31 over the period 2000-2005 at a $0.05^\circ \times 0.05^\circ$ spatial resolution. We find that the new version of TEM
32 made improvement over the previous version and generally captured the expected temporal and spatial
33 patterns of regional carbon dynamics. We estimate that regional GPP is between 7.02 and 7.78 Pg C yr⁻¹
34 and net primary production (NPP) ranges from 3.81 to 4.38 Pg C yr⁻¹ and net ecosystem production
35 (NEP) varies within 0.08-0.73 Pg C yr⁻¹ over the period 2000-2005 for the conterminous United States.
36 The uncertainty due to parameterization is 0.34, 0.65 and 0.18 Pg C yr⁻¹ for the regional estimates of
37 GPP, NPP and NEP, respectively. The effects of extreme climate and disturbances such as severe
38 drought in 2002 and destructive Hurricane Katrina in 2005 were captured by the model. Our study
39 provides a new independent and more adequate measure of carbon fluxes for the conterminous United
40 States, which will benefit studies of carbon-climate feedback and facilitate policy-making of carbon
41 management and climate.

42 **Keywords:** Carbon dynamics; Terrestrial Ecosystem Model; Remote Sensing; MODIS; EVI; LSWI;

43 AmeriFlux

44

45 **1. Introduction**

46 Quantification of net carbon exchanges between the terrestrial ecosystems and atmosphere is
47 scientifically and politically important. It can help improve our understanding of the feedbacks between
48 the terrestrial biosphere and atmosphere (Law et al., 2006) and provide critical information to studying
49 long-term biosphere interactions with other components of the Earth system (Potter et al., 2007). The
50 Intergovernmental Panel on Climate Change (IPCC) reported that the continent of North America has
51 been identified as a significantly large fraction of global carbon budget in terms of both source and sink
52 of atmospheric CO₂ (Pacala et al., 2001;Gurney et al., 2002;IPCC, 2001). The conterminous United
53 States accounts for most of the North American total, but with a high uncertainty. For instance, Pacala et
54 al. (2001) estimated a carbon sink in the conterminous United States is between 0.30 and 0.58 Pg C
55 yr⁻¹ (1 Pg = 10¹⁵ g) over the 1980s. Fan et al. (1998) estimated the North America sink as 1.7 ± 0.5 Pg C
56 yr⁻¹ over the period of 1988 to 1992, mostly in the south of 51° N. Analyses based on land use change
57 and inventory databases for the conterminous United States in the 1980s estimated a sink of 0.08 to 0.35
58 Pg C yr⁻¹ (Turner et al., 1995;Houghton et al., 1999;Houghton and Hackler, 2000;Houghton et al., 2000).
59 Results from the Vegetation/Ecosystem Modeling and Analysis Project (VEMAP) suggested a smaller
60 sink (0.08 ± 0.02 Pg C yr⁻¹) of the conterminous United States from 1980 to 1993 (Schimel et al., 2000).
61 Recently, Potter et al. (2007) estimated a sink of 0.04 to 0.2 Pg C yr⁻¹ from 2000 to 2004 while Xiao et al.
62 (2008) estimated the sink at 0.68 Pg C yr⁻¹ over the period 2000 to 2006 using satellite information.
63 Overall, these results have shown great uncertainties, and remarkably, the uncertainty sometimes is
64 larger than the sink itself.

65 Reducing the uncertainty of large-scale carbon exchanges requires more adequate
66 comprehension to the related biophysical processes. Traditionally, process-based biogeochemical

67 models have been used (e.g. Raich et al., 1991;Potter et al., 1993;Field et al., 1995;Zhuang et al.,
68 2003;Running and Hunt, 1993). These models usually consider carbon fluxes as functions of climatic
69 and biogeochemical factors (McGuire et al., 1992) and are able to estimate carbon fluxes and storage in
70 the ecosystem. However, since the environmental limitation for simulating carbon fluxes is estimated
71 with specific algorithms driven by uncertain environmental variables, biases between the observed and
72 estimated environmental status can introduce uncertainty. In addition, terrestrial biogeochemical model
73 simulations are uncertain due to lacking of large-scale disturbance data (Canadell et al., 2000;Law et al.,
74 2006). Remotely sensed data provide globally consistent and near real-time observations of numerous
75 surface variables as well as the information of the timing, distribution, spatial extent or severity of
76 disturbances at regional and global scales (Zhao and Running, 2008). These satellite data help more
77 adequately quantify carbon dynamics (Coops et al., 1998;Seaquist et al., 2003;Xiao et al., 2004;Sims et
78 al., 2008). These remotely-sensed data are good at estimating carbon assimilation and plant respiration,
79 but not heterotrophic respiration. Satellite-based models alone cannot sufficiently account for
80 vegetation carbon (Xiao et al., 2010) and nitrogen availability (Clark et al., 1999;Clark et al., 2004)
81 while these can be provided by process-based models. Therefore, models that are based on both satellite
82 observations and biogeochemical processes could potentially improve the quantification of carbon
83 dynamics of Gross Primary Production (GPP), Autotrophic Respiration (R_A) and heterotrophic
84 respiration (R_H). For example, Potter et al. (2003) retrieved major disturbances at a global scale with
85 the AVHRR FPAR data for the period of 1982-1999 and combined them with the NASA-CASA model
86 to estimate the above-ground biomass carbon lost. Hazarika *et al.* (2005) used MODIS derived Leaf
87 Area Index (LAI) to constrain an ecosystem model (Sim-CYCLE) and improved the accuracy in
88 estimating global Net Primary Production (NPP). However, limitations still exist in those studies. For

89 example, the NASA-CASA directly modeled NPP but avoided the estimation of the Gross Primary
90 Production (GPP). The MODIS LAI products used for constraining Sim-CYCLE are not directly
91 calculated with surface reflectance but derived with complex algorithms (Myneni et al., 2002) which
92 can cause high uncertainty. Here we conduct a study by combining satellite reflectance data with a
93 process-based biogeochemistry model, the Terrestrial Ecosystem Model (McGuire et al., 2001; Zhuang
94 et al., 2003; McGuire et al., 1992; Raich et al., 1991), to quantify the carbon dynamics in the
95 conterminous U.S. for the period of 2000-2005.

96 Eddy covariance flux towers have been established since the 1990s to provide continuous
97 measurements of ecosystem-level carbon exchanges (Wofsy et al., 1993; Baldocchi et al., 2001). At
98 present, over 400 eddy covariance flux towers are operating on a long-term and continuous basis over
99 the globe (FLUXNET, 2009). This global network covers a wide range of climate and biome types, and
100 provides probably the best measurements of Net Ecosystem carbon Exchange (NEE) (Xiao et al., 2008).
101 Previous ecosystem models were either estimated or calibrated with annual values of observed carbon
102 fluxes (Raich et al., 1991; Potter et al., 1993) and the time series data of carbon fluxes have not been
103 adequately used. In recent years, a number of studies used eddy flux data in a model-data fusion
104 manner to improve the parameterization and predictability of process-based ecosystem models (e.g.
105 Tang and Zhuang, 2008; Braswell et al., 2005; Williams et al., 2005; Aalto et al., 2004; Santaren et al.,
106 2007; Tang and Zhuang, 2009; Wang et al., 2007; Wang et al., 2001). Here we conduct a model-data
107 fusion study with a satellite-based model. We first develop a new version of TEM based on
108 satellite-observed surface reflectance, which is hereafter referred to as SAT-TEM. Second we
109 parameterize the SAT-TEM using flux tower data and compare both SAT-TEM and TEM performance
110 at the site level. Finally, we use SAT-TEM to quantify carbon fluxes in the conterminous United States

111 in comparison with the estimates of a previous version of TEM.

112

113 **2. Method**

114 *2.1. Overview*

115 In this study, Enhanced Vegetation Index (EVI) and Land Surface Water Index (LSWI) from
116 Moderate Resolution Imaging Spectroradiometer (MODIS), which are of high data quality and
117 accuracy (Justice et al., 2002;Guenther et al., 2002;Wolfe et al., 2002), are incorporated into the
118 process-based biogeochemistry model TEM. Observed data from AmeriFlux sites (AmeriFlux, 2009)
119 are then utilized to improve parameterization of the model and test the model performance. Specifically,
120 we modify GPP formulae in TEM by incorporating MODIS EVI and LSWI. We then use a Bayesian
121 Inference technique (Tang and Zhuang, 2009) to parameterize the model. The model is then verified for
122 different ecosystem types with the observed Net Ecosystem Exchange (NEE) and GPP from eddy
123 covariance flux towers of AmeriFlux network. To examine how the new model could improve the
124 carbon flux estimation of TEM, we run both versions of TEM at the same sites with the same driving
125 data sets. The model is finally applied to estimate dynamics of carbon fluxes for each $0.05^{\circ} \times 0.05^{\circ}$ grid
126 cell across the conterminous United States over the period 2000-2005.

127

128 *2.2. Modification to the Terrestrial Ecosystem Model*

129 The TEM is a well-documented process-based ecosystem model that describes carbon and
130 nitrogen dynamics of plants and soils for terrestrial ecosystems (Raich et al., 1991;McGuire et al.,
131 1992;McGuire et al., 2001;Melillo et al., 1993;Zhuang et al., 2001;Zhuang et al., 2002;Zhuang et al.,

132 2003;Zhuang et al., 2004). The TEM runs at monthly time step and uses spatially referenced
133 information on climate, elevation, soils, vegetation and water availability as well as soil- and
134 vegetation-specific parameters to make monthly estimates of important carbon and nitrogen fluxes and
135 pool sizes of terrestrial ecosystems. In TEM, GPP is modeled as a function of irradiance of
136 photosynthetically active radiation (PAR), atmospheric CO₂ concentrations, moisture availability, mean
137 air temperature, the relative photosynthetic capacity of the vegetation, and nitrogen availability. The
138 freezing and thawing dynamics have also been considered (Zhuang et al., 2003). The formula for
139 calculating monthly GPP is:

$$140 \quad GPP = C_{max} f(PAR) f(PHENOLOGY) f(FOLIAGE) f(T) f(C_A, G_v) f(NA) f(FT) \quad (1)$$

141 where C_{max} is the maximum rate of C assimilation by the entire plant canopy under optimal
142 environmental conditions; $f(PAR)$ represents the influence of photosynthetically active radiation;
143 $f(PHENOLOGY)$ is monthly leaf area relative to leaf area during the month of maximum leaf area
144 depending on monthly estimated evapotranspiration (Raich et al., 1991); $f(FOLIAGE)$ is a scalar
145 function representing the ratio of canopy leaf biomass relative to maximum leaf biomass (Zhuang et al.,
146 2002) having the similar effect as $f(PHENOLOGY)$ on constraining the estimation of GPP; $f(T)$ is
147 temperature scalar with reference to the derivation of optimal temperatures for plant production and T is
148 monthly air temperature; $f(C_A, G_v)$ represents the effect of CO₂ concentrations, where C_A is CO₂
149 concentration in the atmosphere and G_v is a unitless multiplier that accounts for changes in leaf
150 conductivity to CO₂ resulting from changes in moisture availability. The function $f(NA)$ models the
151 limiting effects of plant nitrogen availability. $f(FT)$ is an index of sub-monthly freeze-thaw to indicate
152 effects of freeze-thaw dynamics on GPP (Zhuang et al., 2003). In TEM, NPP is defined as the difference
153 of GPP and autotrophic respiration (R_A) and the net carbon exchange between the ecosystems and

154 atmosphere is defined as NEP, a difference between NPP and heterotrophic respiration (R_H) (Raich et al.,
155 1991;McGuire et al., 1992;McGuire et al., 2001;Zhuang et al., 2003).

156 Satellite vegetation indices are widely used in satellite-based carbon models to represent the
157 fraction of vegetation absorbed PAR (FAPAR) (Prince and Goward, 1995; Running et al., 1999, 2000,
158 Potter et al., 1993; Xiao et al., 2004). For example, the Normalized Difference Vegetation Indices
159 (NDVI), which captures the contrast between the visible-red and near-infrared reflectance of vegetation,
160 has a good linear or non-linear relationship of FAPAR. Recent studies show that EVI (Huete et al.,
161 1997;Huete et al., 2002) calculated from the MODIS could more efficiently dismiss the influence of
162 atmospheric scattering and sensitive to canopy variations (Huete et al., 2002). EVI is believed to be a
163 better choice than NDVI to represent photosynthetic activity of vegetation canopy (Boles et al.,
164 2004;Xiao et al., 2004;Yang et al., 2007) and provides reasonably accurate direct estimates of GPP
165 (Rahman et al., 2005). EVI is a normalized index using the reflectance in the near infrared (NIR), red
166 and blue spectral bands:

$$167 \quad EVI = \frac{2.5(\rho_{nir} - \rho_{red})}{\rho_{nir} + (6\rho_{red} - 7.5\rho_{blue}) + 1} \quad (2)$$

168 Apart from EVI, Xiao et al. (2004) developed the Vegetation Photosynthesis Model (VPM)
169 which used the Land Surface Water Index (LSWI) to help capture the effects of water stress and leaf
170 phenology. As the shortwave infrared (SWIR) spectral band is sensitive to land surface water content,
171 the LSWI is calculated as the normalized difference between NIR and SWIR spectral bands:

$$172 \quad LSWI = \frac{\rho_{nir} - \rho_{swir}}{\rho_{nir} + \rho_{swir}} \quad (3)$$

173 where the SWIR spectral bands may be either 1628–1652 nm or 2105–2155 nm for MODIS on
174 board the NASA Terra satellite (Yan et al., 2009;Ratana et al., 2005;Li et al., 2007). In our study, we use

175 the band at 2105–2155 nm to calculate LSWI.

176 We therefore adopt the formulae of the VPM for GPP modeling in our revision of TEM. We use
177 water scalar (W_{scalar}), phenology scalar (P_{scalar}) and EVI to account for the vegetation water stress and
178 phenology as well as absorption of PAR while maintaining the original formulation for nitrogen
179 availability, temperature constraints, and the effect of CO₂ concentration. GPP in the new version of
180 TEM (SAT-TEM) is thus modeled as:

$$181 \quad GPP = C_{\text{max}} f(\text{PAR}) f(T) W_{\text{scalar}} P_{\text{scalar}} f(C_A, G_v) f(\text{NA}) f(\text{FT}) \quad (4)$$

182 where $f(\text{PAR}) = \text{EVI} \times \text{PAR} / (k_i + \text{PAR})$ indicates the PAR absorption and the effect of PAR
183 saturation while k_i is the half-saturation value. $W_{\text{scalar}} = (1 + \text{LSWI}) / (1 + \text{LSWI}_{\text{max}})$ where LSWI_{max} is the
184 maximum LSWI within the plant-growing season for individual grid cell. Through our study, we
185 calculated LSWI_{max} in advance and use it as an input parameter for each grid cell in the regional
186 simulation. $P_{\text{scalar}} = (1 + \text{LSWI}) / 2$. Specifically, P_{scalar} is set to be 1 for evergreen vegetations (Xiao et al.,
187 2004). The calculations of NPP and NEP in SAT-TEM are kept the same as the previous version of
188 TEM.

189

190 2.2 Data Organization

191 2.2.1. Site-level data

192 To drive SAT-TEM model, we first parameterize SAT-TEM using AmeriFlux site observations.
193 We organize the observed GPP, NEP and meteorological data (radiation, air temperature, and
194 precipitation) from six representative eddy covariance flux sites for each vegetation type to
195 parameterize and verify SAT-TEM. In order to further test the performance of SAT-TEM, we organize
196 the same data from ten additional available sites covering all the six vegetation types across most of the

197 conterminous United States (Figure 1). Specifically, we gather all available monthly Level 4 GPP and
198 Net Ecosystem Exchange (NEE) products (<http://public.ornl.gov/ameriflux/>) at these sites (Table 1).
199 The Level 4 product consists of two types of NEE data, including standardized (NEE_st) and original
200 (NEE_or) NEE. Corresponding GPP_st and GPP_or are calculated by ecosystem respiration (R_e) with
201 NEE_st and NEE_or, respectively. GPP_st, GPP_or, NEE_st and NEE_or are filled using the Marginal
202 Distribution Sampling (MDS) method (Reichstein et al., 2005) and the Artificial Neural Network (ANN)
203 method (Papale and Valentini, 2003). We use GPP and NEE calculated from NEE data that were
204 gap-filled using the ANN method (Moffat et al., 2007; Xiao et al., 2008). For each site, if the percentage
205 of the remaining missing values for NEE_st is lower than that for NEE_or, we select NEE_or and
206 GPP_or; otherwise, we use NEE_st and GPP_st. To compare with our TEM simulation, we treat NEE as
207 TEM NEP, but with different signs.

208 We obtain site-level EVI and LSWI by collecting MODIS ASCII subsets (Collection 5) which
209 consist of $7 \text{ km} \times 7 \text{ km}$ regions centered on the flux tower from the Oak Ridge National Laboratory's
210 Distributed Active Archive Center for each AmeriFlux site. This 16-day product has a spatial resolution
211 of $1 \text{ km} \times 1 \text{ km}$. To better represent the flux tower footprint (Schmid, 2002; Rahman et al., 2005; Xiao et
212 al., 2008; Xiao et al., 2010), mean EVI, NIR and SWIR band values for the central $3 \text{ km} \times 3 \text{ km}$ area are
213 extracted within the $7 \text{ km} \times 7 \text{ km}$ cutouts. We only use the pixels with good quality which are
214 determined by the corresponding quality assurance (QA) flags included in the product. LSWIs are then
215 calculated by NIR and SWIR band values. Each 16-day EVI and LSWI values are aggregated into
216 monthly values to correspond with the time step of SAT-TEM.

217

218 *2.2.2. Regional spatially-explicit data*

219 To conduct regional simulations, we organize the regional data of vegetation, soils, topography,
220 and climate at a spatial resolution $0.05^\circ \times 0.05^\circ$. We obtain land-cover information derived from
221 MODIS product Land Cover Types Yearly L3 Global 0.05 Deg CMG (MOD12C1) (Year 2004) from
222 NASA Goddard Space Flight Center website (<http://modis-land.gsfc.nasa.gov>). We use the
223 classification of the International Geosphere and Biosphere (IGBP) land-cover classification system to
224 classify the land cover map of the conterminous United States into 6 major vegetation types, which are
225 used in our SAT-TEM simulations (Table 2 and Figure 1). EVI, NIR and SWIR bands data are extracted
226 from MOD13C2 (MODIS Terra Vegetation Indices Monthly L3 Global 0.05Deg CMG V005) for the
227 conterminous United States.

228 Mean monthly climate data including air temperature, cloudiness fractions and precipitation are
229 extracted from NCEP global datasets at a 0.5° spatial resolution (Kistler et al., 2001). Spatial elevation
230 data and soil texture data from previous studies are from Zhuang et al. (2003). All these data are
231 interpolated into a 0.05° spatial resolution using Inverse Distance Weighted method to match MODIS
232 data.

233

234 *2.3 Model Parameterization and Application*

235 We parameterize the SAT-TEM with a Bayesian inference method (Tang and Zhuang, 2009) at
236 the selected six AmeriFlux sites representing every major vegetation type across the conterminous
237 United States. The parameterization method follows the procedures described in Tang and Zhuang
238 (2009). Firstly, 15 key parameters (Table 3) are selected to conduct the parameterization according to
239 our previous sensitivity study (Tang and Zhuang, 2009) and parameterization experiences. To derive
240 the prior parameter sets of SAT-TEM, we first assume that they follow the uniform distributions within

241 previous specified reasonable ranges either based on literature review or our experience. We sample
242 500,000 sets of parameters using the Latin Hypercube Sampling technique (Iman and Helton, 1988) to
243 conduct the Monte Carlo simulations. We then use the sampling importance resampling (SIR)
244 technique with the observed carbon fluxes at the selected sites to draw the posterior from the prior
245 SAT-TEM simulations (Skare et al., 2003) and collect 50,000 posterior sets of parameters, which are
246 one-tenth of the prior sample size and are suggested to be able to produce stable results (Green et al.,
247 1999; Tang and Zhuang, 2009). We then divide the errors made by the 50,000 sets of parameters into 50
248 levels (from the highest error level to the lowest) and sampled 50 sets of parameters, one for each level.
249 These 50 sets of parameters are applied at both sites and the region for ensemble simulations of
250 SAT-TEM to account for the uncertainties of parameterization at different spatial scales. Here the first
251 2-year data at all the six sites are used for parameterization while data of the remaining years are used
252 for testing the model. To further test the performance of the SAT-TEM and compare it with TEM
253 independently apart from the parameterization sites, we run both SAT-TEM and TEM at ten additional
254 AmeriFlux sites which represent all six vegetation types within diverse climatic zones across the
255 conterminous United States. Statistics of R^2 and Root Mean Square Error (RMSE) are calculated to
256 quantitatively evaluate the model performance. The TEM parameters for natural ecosystems are from
257 previous studies (McGuire et al., 1992; Zhuang et al., 2003), parameters for croplands are averaged
258 values for C_3 and C_4 plants from (Lu and Zhuang, 2010).

259 The parameterized SAT-TEM is then applied to the conterminous United States for the period
260 of 1948-2005 at a 0.05° spatial resolution with a total of 322287 grid cells. We first run SAT-TEM to
261 equilibrium with the long-term averaged climate and CO_2 concentration data from 1948 to 2005. We
262 then spin-up the model for 120 years to account for the influence of climate inter-annual variability on

263 the initial conditions of the ecosystems. Since historic climate and CO₂ concentration data are not
264 available before 1948, we repeat the data from 1948 to 1987 for three times for the spin-up. In addition,
265 since MODIS vegetation index products are only available from 2000, we fill the gap by repeating
266 2000-2005 MODIS EVI data for the whole period in order to have consistent data for our simulation
267 period. After the spin-up, we run the model with transient monthly climate and annual atmospheric CO₂
268 concentrations from 1948 to 2005 and then extract the results of the period of 2000-2005 for further
269 analysis. To quantify the uncertainty of regional simulation caused by parameterization, we run
270 ensemble SAT-TEM simulations with the 50 sets of parameters obtained from site-level
271 parameterizations. The averaged values and standard deviations of 50 sets of regional results are
272 calculated for analysis. For comparison, we also conduct a regional simulation with TEM.

273

274 **3. Results and Discussion**

275 *3.1 Model Performance at AmeriFlux Sites*

276 The parameterized SAT-TEM can reproduce the carbon fluxes reasonably well at the six
277 parameterization sites. Comparisons at each individual site show reasonable agreement of seasonality
278 and inter-annual variability between the observed and predicted values (Figure 2, Table 4) except for
279 Sky Oaks New site. Specifically, at forest sites, SAT-TEM simulations better capture the variation of
280 both fluxes of GPP and NEP ($R^2 > 0.9$ for GPP and $R^2 > 0.6$ for NEP) when comparing to non-forest
281 sites. SAT-TEM results at Sky Oaks New site however have a relatively lower linear relationship ($R^2 =$
282 0.10 for GPP and $R^2 = 0.13$ for NEP) comparing to $R^2 > 0.7$ for GPP at other sites. Literature review
283 (Xiao et al., 2008, 2010; Sims et al., 2008) shows previous satellite-based estimations all failed to
284 capture the variation of carbon fluxes at this site. Apart from the reason of short records at this site, this

285 disagreement is likely due to solar elevation angle effects on spectral reflectance (Sims et al., 2008)
286 since it is reported that surface reflectance as well as NDVI and EVI are strongly affected by diurnal and
287 seasonal changes in solar elevation angle when vegetation is sparse (Goward and Huemmrich,
288 1992;Pinter et al., 1983, 1985;Sims et al., 2006, 2008). There is also a relatively weak linear
289 relationship between SAT-TEM NEP and observations at Tonzi Ranch site. This may be due to MODIS
290 and tower footprints that do not match with each other at this site according to Ma et al., (2007) and
291 Xiao et al., (2008). Tonzi Ranch site is dominated by deciduous blue oaks and the understory while the
292 MODIS footprint consists of larger area of grassland. Since the phenology of these two ecosystems is
293 distinct from each other, they contribute differently to the integrated fluxes, leading to the error of
294 model predictions.

295 Overall, performance of SAT-TEM is obviously superior to that of TEM as shown in Table 4 at
296 the six parameterization sites. Statistics of SAT-TEM results have notable higher R^2 values and lower
297 RMSE at all these sites showing that SAT-TEM has better ability to capture the variations and
298 magnitudes of both GPP and NEP fluxes. The superiority of SAT-TEM is especially reflected at the
299 non-forested sites considering the corresponding poor performances of TEM. This finding may indicate
300 that TEM is better at simulating forest fluxes but weaker at simulating the seasonality and variations of
301 carbon sequestration in non-forested ecosystems where satellite observations may provide a significant
302 help.

303 Testing at the other ten additional sites generates the similar results (Figure 3, Table 5).
304 Comparing to the non-forested sites, both SAT-TEM and TEM have promising simulations at the
305 forested sites and SAT-TEM performs overall better than TEM with significantly higher values of R^2
306 and lower values of RMSE. SAT-TEM again shows superior performances to TEM at the non-forested

307 sites. Except the shrubland site, the averaged R^2 of SAT-TEM GPP and NEP at all non-forested sites are
308 0.68 and 0.27, respectively. Comparing to 0.41 and 0.12 of TEM, SAT-TEM can better capture the
309 seasonality and inter-annual variability of the carbon fluxes than TEM. SAT-TEM's RMSEs are much
310 lower than TEM's at these sites, indicating that SAT-TEM has better performance. Both SAT-TEM
311 and TEM do not perform well at the only available shrubland site. The Sky Oaks Old site is very close
312 to the parameterization sites, thus the verification result is similar at the parameterization site. However,
313 SAT-TEM still performs better with higher R^2 and lower RMSE for both GPP and NEP. The high
314 RMSEs at cropland sites are probably due to the different crop species, the rotations of different crops
315 and the different field managements, which have not been considered in simulations.

316 SAT-TEM estimated GPP and NEP are under- or over-predicted for some sites. The model
317 could not capture exceptionally high values in the summer at some sites, such as some summer months
318 at the cropland sites (Bondville, Rosemount, Mead Irrigated). Underestimations of NEP also take place
319 in the winters at the Howland site, the springs and the winters at the Wind River Crane site, possibly due
320 to the overestimation of the ecosystem respirations at these two sites. The model also overestimated
321 GPP at the Varia Ranch site in winters. Considering the low quality of GPP in winters (most of them < 0),
322 our estimation could still be in a reasonable range. If we pool all the measured fluxes together (Figure
323 4), SAT-TEM shows better performance.

324 We find the errors introduced by parameterization are relatively small at most sites except at the
325 shrubland sites and evergreen forest sites with SAT-TEM (Figure 2 and 3). The most significant errors
326 are usually occurring in summer commonly with relatively higher air temperature and abundant solar
327 radiation, and precipitation, which can amplify the differences (Tang and Zhuang, 2009, 2008).
328 Comparing to GPP, the simulated NEP has more significant errors, which is probably due to the error

329 propagation when more parameters are involved in NEP calculation.

330

331 *3.2 Temporal variation of carbon fluxes in the conterminous U.S.*

332 Annual GPP, NPP and NEP for the conterminous United States over the period 2000-2005 vary
333 from year to year (Table 6). Discrepant results are found comparing to previous studies in the same
334 region and similar time period (Table 7). The SAT-TEM estimated GPP flux varies from 7.02 to 7.78 Pg
335 C yr⁻¹ with of an annual average 7.43 Pg C yr⁻¹. This estimate is close to 7.06 Pg C yr⁻¹ estimated by
336 (Xiao et al., 2010) over the period 2001-2006 but higher than 6.2 Pg C yr⁻¹ of MODIS GPP product
337 (Zhao et al., 2005) for the period of 2000-2005. Our estimate NPP ranges from 3.81 to 4.38 Pg C yr⁻¹ in
338 this period, which is much higher than the range of 2.67-2.79 Pg C yr⁻¹ over 2000-2004 from Potter et al.,
339 (2007) and the 3.3 Pg C yr⁻¹ from MODIS NPP product over 2000-2005(Zhao et al., 2005). Our
340 estimated NEP is 0.08-0.73 Pg C yr⁻¹ with an average 0.41 Pg C yr⁻¹. Overall our estimations are higher
341 than 0.04-0.2 Pg C yr⁻¹ from Potter et al., (2007), and much lower than the estimates as high as 1.21 Pg
342 C yr⁻¹ from Xiao et al. (2011) but our estimation of 0.40 Pg C yr⁻¹ in 2003 is closer to the estimate of
343 0.63 Pg C yr⁻¹ based on an inverse modeling approach (Deng et al., 2007). Comparing to NEP in the
344 1980s, SAT-TEM estimated a much higher sink than the VEMAP estimate, which put the sink as 0.08 ±
345 0.02 Pg C yr⁻¹, and the land-based analyses (0.08 - 0.35 Pg C yr⁻¹) (Turner et al., 1995; Houghton et al.,
346 1999, 2000), but close to the results (0.30 - 0.58 Pg C yr⁻¹) provided by Pacala et al. (2001).

347 SAT-TEM NEP has the similar inter-annual variation to the results presented by Potter et al.
348 (2007) and Xiao et al. (2011) which are higher in 2001, 2003 and 2004 but lower in 2000 and 2002.
349 From 2000 to 2003, the whole region acted as a relatively low net sink of atmosphere CO₂ because large
350 area carbon source occurred (Figure 5). Specifically, in 2000, large carbon sources mainly took place in

351 the south central and southwest area. In 2001, part of the Midwest and South Central, the Rocky
352 Mountain area as well as the Pacific Southwest acted as carbon source. In 2002, large area of the
353 Midwest, the Great Plains and the western U.S. were carbon sources. In 2003, carbon sources mainly
354 took place in the western U.S., the Rocky Mountain areas and some part of the east and southeast coast.
355 Except for the near-consistent carbon source in the Rocky Mountain area which is very likely due to
356 cool or cold weather of the highland climate, temperature changes and extreme droughts might be the
357 reason causing the other large area of carbon sources in these years. The National Climatic Data Center
358 (NCDC, <http://www.ncdc.noaa.gov/oa/ncdc.html>) reported that the contiguous U.S. was very warm
359 during the summer but very cold in November and December in 2000. Southwest states such as Utah,
360 New Mexico and Nevada experienced the second or the third warmest year on record. Apart from the
361 abnormal temperature, the drought in 2000 severely affected much of the southern and western U. S.
362 and therefore reduced the carbon uptake and enhanced the intensity of carbon source. In 2001, the
363 Midwest and Pacific Southwest both had abnormally high temperatures. 2003 was reported as the 20th
364 warmest year on record for the United States. Western regions were reported as much warmer than
365 average for the summer. The Northwest Region had its second warmest summer on record, and the
366 Southwest and West had their third in 2003. Abnormally high air temperature significantly enhances
367 ecosystem respirations but does not contribute much to carbon uptake because the temperature may
368 have passed the range of optimums temperature for plant photosynthesis during the summer time.
369 Consequently, the ecosystem acts as a low sink or becomes a carbon source. Year 2002 had the lowest
370 GPP, NPP and NEP during this period. 2002 was an extreme drought year, in which precipitation was
371 lower than 30-year mean annual value. As the year began, moderate to extreme drought covered
372 one-third of the contiguous United States including much of the eastern seaboard and northwestern

373 United States. The combination of generally warmer- and drier-than-average conditions led to a large
374 area of carbon source in 2002 (Figure 5). In addition to the limitations of the carbon uptake, the extreme
375 drought also significantly enhanced the respiration and therefore led to a more severe carbon source.
376 These results suggest that the use of EVI and LSWI is able to reflect the real large-scale environmental
377 conditions and to constrain the estimates of carbon fluxes.

378 In contrast, the year 2004 had slightly above-average temperatures and was the 6th wettest year
379 on record of the nation (NCDC 2004). The year 2005 was above-average warm but had much lower
380 than average temperatures along the Eastern Seaboard in growing season and the precipitation was near
381 the long-term mean of precipitation in the nation (NCDC 2005). These climate patterns resulted in a
382 high sink in these 2 years and a carbon source in the eastern regions in 2005.

383 Seasonality of net carbon uptake of the conterminous United States differed from year to year
384 (Figure 6a). The accumulative NEP of 2002 didn't reach a positive value until early July, which is about
385 one month later than the other years probably due to the severe drought in the spring and summer. Both
386 2004 and 2005 achieved positive accumulative NEP in the early June while the dates for 2000, 2001 and
387 2003 were in the midst June. For most of the years, the accumulative NEP started to increase since April,
388 while the date for 2004 is March, indicating the year 2004 turned from a carbon source into a sink
389 earlier than the other years. Accumulative NEP started to decrease in September for all of the years
390 except 2005, which continued to assimilate more carbon than that was released in October and then
391 reverted to a source. The early-beginning and late-ending growing seasons for the year 2004 and 2005
392 led to much higher annual NEP than the other years. Overall, the carbon budget level of the
393 conterminous United States ecosystems can be classified into 3 groups: high sinks in 2004 and 2005,
394 moderate sinks in 2000, 2001, and 2003, and low sink in 2002.

395 The seasonality of the regional net carbon uptake can be explained by the satellite-observed
396 vegetation indices. The monthly regional averaged EVI and LSWI vary from year to year (Figure 6b,
397 c). EVI generally indicates the greenness of the land surface vegetation and shows the pattern of
398 vegetation green-up and senescence. The patterns of regional averaged EVI were similar for the 6 years
399 but the year 2002 had lower EVI during the green-up period in the spring and the year 2000 had
400 relatively lower EVI during the senescent season. The lower EVI of these two years were reflected by
401 the relatively low NEP in these two years. Particularly, since 2002 was the lowest-sink year, our result
402 may suggest that abnormal EVI in the green-up season led to a stronger influence on the annual total
403 NEP. In contrast, EVI of the year 2004 and 2005 were mostly higher than that of the other years,
404 especially during the summer, which resulted in the highest carbon sink over the 6-year period. Similar
405 to EVI, the low LSWI from April to August in 2002 indicates that the year 2002 was a drought year and
406 the highest LSWI occurred in the main growing seasons in the years 2004 and 2005, leading to a lower
407 and higher net carbon uptake in the year 2002 and the years 2004 and 2005, respectively. The lowest
408 accumulative EVI and LSWI for the other 5 years except 2002 in June were 1.40 and 1.53, while the
409 values in 2002 were 1.40 and 1.39, respectively. In 2002, the accumulative EVI and LSWI were 1.76
410 and 1.77 in July, respectively, which exceeded the levels in June of the other years and the region turned
411 into a carbon sink. These suggest that both EVI and LSWI affect the transition of a carbon source to a
412 sink.

413 Regional estimations between SAT-TEM and TEM differ greatly. The averaged differences
414 are more than 2 and 1.4 Pg C yr⁻¹ for GPP and NPP, respectively. NEP of SAT-TEM is 0.23 Pg C yr⁻¹
415 higher than that of TEM. The simulated interannual variations between these two versions of TEM are
416 also different. Specifically, SAT-TEM indicated the annual carbon fluxes increased in 2000 and 2001

417 and dropped to the lowest values in 2002, then kept increasing in the following years and reached the
418 peak values in 2004 and 2005. In contrast, TEM suggested the highest and lowest GPP and NPP
419 occurred in 2005 and 2000, respectively, and the highest NEP in 2003. During these years, TEM might
420 over- or underestimate the water stress and PAR absorption of the vegetation and therefore provided
421 different carbon sequestration estimations, while SAT-TEM used the satellite information of vegetation
422 index and land surface water index, which constrained the carbon flux estimates. SAT-TEM's
423 performance also benefits from the way of parameterization using the monthly eddy fluxes while TEM
424 was calibrated using annual fluxes only.

425

426 *3.3 Spatial Variation of Carbon Fluxes in the Conterminous U.S.*

427 SAT-TEM simulated annual carbon fluxes generally capture the expected spatial patterns
428 (Figure 7). GPP and NPP have a similar spatial variability from west to east across the conterminous
429 United States. The West Coast, which is dominated by evergreen forest, has high annual GPP and NPP.
430 The western Great Plains and the Rocky Mountain as well as the Southwest regions have relatively low
431 GPP and NPP owing to sparse vegetation and arid climate. Cropland areas in the Midwest have
432 relatively high GPP and NPP probably due to ample irrigation and fertilization. Highest GPP and NPP
433 occur in the east United States with dense vegetation. The Gulf Coast has especially high GPP mainly
434 due to its favorable temperature and abundant precipitation.

435 Most areas across the conterminous United States have positive NEP from 2000 to 2005. Most
436 forested areas are carbon sinks and the highest sinks take place in the woody regions in the eastern
437 United States and especially in the Northeast with intensive radiation, abundant precipitation, warm
438 temperature or dense vegetation cover. But the carbon sources also take place in forest regions, mostly

439 in the south Rocky Mountain area and Sierra Nevada Mountain mainly due to the cold and dry climate.
440 Non-forest regions including grassland, savannas, shrubland as well as cropland act as a carbon sink.
441 Except the year 2000, most area of grassland in the south especially in Texas is a persistent carbon sink
442 with warm weather and abundant precipitation with 100 to $250 \text{ g C m}^{-2} \text{ yr}^{-1}$ over the 6-year period. Most
443 cropland areas are carbon sinks with the intensity of 50 to $100 \text{ g C m}^{-2} \text{ yr}^{-1}$.

444 Carbon dynamics vary in different ecosystems (Table 8). Cropland contributes the most to the
445 conterminous United States carbon sink with the highest GPP, NPP and NEP. Forests follow cropland
446 to have high total GPP, NPP and contribute about one-third of the total net carbon uptake. With the
447 second largest area, grasslands contribute about one-sixth to one-fifth of total annual GPP and NPP, and
448 one-sixth of total annual NEP. Shrubland has the lowest total annual GPP, NPP while savannas have the
449 lowest total annual NEP. On a per-unit area basis, forests have the highest GPP, following with cropland
450 and savannas. Deciduous forests have the highest NPP intensity while shrubland and grasslands have
451 the lowest. Deciduous forest NEP is the highest and shrubland have the lowest carbon sink. Overall,
452 deciduous forests and croplands are the main contributors to the national carbon sink over the period
453 2000-2005.

454 Since the disturbance damages to vegetation can be reflected by the variations of EVI, use of
455 EVI in TEM helps capture the effects of disturbances on carbon dynamics. For example, the Hurricane
456 Katrina occurred in late August 2005 and affected five million acres of forest across Mississippi,
457 Louisiana and Alabama with downed trees, snapped trunks and broken limbs to stripped leave.
458 Dramatic changes of EVI occurred in the following two months (September and October) after the
459 hurricane in that region. For the most influenced region between $90^{\circ}\text{W}\sim 88^{\circ}\text{W}$ and $29^{\circ}\text{N}\sim 31^{\circ}\text{N}$, the EVI
460 is averagely about 0.04 lower than normal values for each pixel during those two months. SAT-TEM

461 indeed estimated a large negative GPP anomaly in that period (Figure 8). GPP is $14 \text{ g C m}^{-2} \text{ month}^{-1}$
462 lower than normal values for each pixel. In contrast, TEM failed to capture these anomalies and even
463 presented positive anomalies due to the abundant water storage in that period. Our SAT-TEM results
464 agree with the findings suggesting Hurricane Katrina had large impacts on the regional carbon budget
465 based on satellite data and empirical approaches (Chambers et al., 2007; Xiao et al., 2010).

466

467 *3.4 Possible Uncertainties*

468 The data used to drive SAT-TEM and the parameterization both result in uncertainties to our
469 estimation. As indicated by Zhao et al. (2006), the NCEP reanalysis data overestimated solar radiation
470 and underestimated temperature. The errors in temperature may introduce errors in carbon fluxes
471 because of the nonlinear relationship between temperature and plant maintenance respiration. The
472 heterogeneity of land covers is another important source of uncertainty when we scale the site-level
473 parameterization to the region. For example, C_3 and C_4 plants in the regional simulations are not
474 treated differently since there is no transient spatially-explicit C_3 and C_4 plant distribution data.

475 Second, carbon dynamics are uncertain due to lacking spatially-explicit forest stand age data.
476 In this study, we assume that all ecosystems (e.g., forests) are mature. Parameters generated at the
477 chosen matured forest at Howland and Harvard forest sites do not work for young forests. Thus models
478 may underestimate NPP of the forest in the conterminous United States because the forest productivity
479 generally decreases with stand age (McMurtrie et al., 1995). Although the usage of MODIS vegetation
480 indices can represent some information of the forest age (Waring et al., 2006), more adequate
481 quantification of the regional carbon fluxes should use spatially-explicit data of forest stand age.

482 Third, the uncertainty came from a limited number of quality ecosystem sites. For example,

483 there are only a few shrubland sites with sufficient observations. The weak constraint on parameters of
484 SAT-TEM for shrubland may bias the results. In addition, more sites in the western U.S. should be
485 established. The significant uncertainties of eddy flux data (Richardson et al., 2008) and the
486 uncertainties introduced by the gap-filling techniques (Moffat et al., 2007) may also bias
487 parameterization and regional results.

488 Finally, the parameterization could also introduce uncertainty to flux estimates. Here we use
489 the 50 ensemble regional simulations to quantify the errors from parameterization. Parameterizations of
490 different vegetation types contribute differently to the total uncertainties (Figure 7). The spatial
491 distribution of the relative standard deviation, as the ratio of standard deviation to the mean value
492 indicates that shrubland has the biggest uncertainties. Evergreen forests in the Rocky Mountain area
493 and the upper Midwest are the second largest uncertainty contributor. With the Bayesian Inference
494 method (Tang and Zhuang, 2008, 2009), the possible parameter sets introduce 0.34, 0.65 and 0.18 Pg C
495 biases to the estimation of the annual GPP, NPP and NEP of the conterminous United States,
496 respectively (Table 6).

497

498 **4. Conclusions**

499 We incorporate MODIS EVI and LSWI into a process-based biogeochemistry model TEM to
500 more adequately quantify ecosystem carbon dynamics from 2000 to 2005 for the conterminous United
501 States. Multiple eddy flux tower data are used to parameterize and verify the SAT-TEM. Ensemble
502 simulations with the posterior parameters are applied at both site and regional levels. The site-level
503 comparisons indicate that the SAT-TEM performs better. The regional extrapolation of SAT-TEM
504 across the conterminous United States generally captures the expected spatial and temporal carbon

505 dynamics. With SAT-TEM, we estimate that the GPP is between 7.02 and 7.78 Pg C yr⁻¹, NPP varies
506 from 3.81 to 4.38 Pg C yr⁻¹ and NEP ranges from 0.08 to 0.73 Pg C yr⁻¹ in the region during the period
507 2000-2005. The parameterization introduces 0.34, 0.65 and 0.18 Pg C yr⁻¹ errors to the regional GPP,
508 NPP and NEP, respectively. The effects of extreme climate and disturbances such as severe drought in
509 2002 and Hurricane Katrina in 2005 are captured in our regional simulations. This study takes
510 advantage of process-based ecosystem modeling, satellite observations and eddy flux tower carbon flux
511 data to provide a more adequate quantification of carbon fluxes for the conterminous United States. Our
512 findings and carbon flux product should benefit studies of carbon-climate feedbacks and facilitate
513 policy-making of carbon management and climate change.

514

515 **Acknowledgements:** We acknowledge the AmeriFlux community to provide the eddy flux data and the
516 MODIS research community to provide MODIS data on vegetation. This research is supported by NSF
517 through projects of ARC-0554811 and EAR-0630319 and the Department of Energy. The study is also
518 supported by NASA land-use and land-cover change program. Computing support is provided by the
519 Rosen Center for Advanced Computing at Purdue University.

520

521

522 **References:**

- 523 Aalto, T., Ciais, P., Chevillard, A., and Moulin, C.: Optimal determination of the parameters controlling
524 biospheric CO₂ fluxes over Europe using eddy covariance fluxes and satellite NDVI
525 measurements, *Tellus B*, 56, 93-104, 2004.
- 526 AmeriFlux Network, Published at <http://ameriflux.ornl.gov/>, 2009.
- 527 Baldocchi, D., Falge, E., Gu, L., Olson, R., Hollinger, D., Running, S., Anthoni, P., Bernhofer, C., Davis,
528 K., Evans, R., Fuentes, J., Goldstein, A., Katul, G., Law, B., Lee, X., Malhi, Y., Meyers, T.,
529 Munger, W., Oechel, W., Paw, K. T., Pilegaard, K., Schmid, H. P., Valentini, R., Verma, S.,
530 Vesala, T., Wilson, K., and Wofsy, S.: FLUXNET: A New Tool to Study the Temporal and
531 Spatial Variability of Ecosystem-Scale Carbon Dioxide, Water Vapor, and Energy Flux
532 Densities, *Bulletin of the American Meteorological Society*, 82, 2415-2434,
533 doi:10.1175/1520-0477(2001)082<2415:FANTTS>2.3.CO;2, 2001.
- 534 Boles, S. H., Xiao, X., Liu, J., Zhang, Q., Munkhtuya, S., Chen, S., and Ojima, D.: Land cover
535 characterization of Temperate East Asia using multi-temporal VEGETATION sensor data,
536 *Remote Sensing of Environment*, 90, 477-489, 2004.
- 537 Braswell, B. H., Sacks, W. J., Linder, E., and Schimel, D. S.: Estimating diurnal to annual ecosystem
538 parameters by synthesis of a carbon flux model with eddy covariance net ecosystem exchange
539 observations, *Global Change Biology*, 11, 335-355, 2005.
- 540 Canadell, J. G., Mooney, H. A., Baldocchi, D. D., Berry, J. A., Ehleringer, J. R., Field, C. B., Gower, S.
541 T., Hollinger, D. Y., Hunt, J. E., Jackson, R. B., Running, S. W., Shaver, G. R., Steffen, W.,
542 Trumbor, S. E., Valentini, R., and Bond, B. Y.: Carbon metabolism of the terrestrial biosphere :
543 A multitechnique approach for improved understanding, 2, Springer, New York, NY,
544 ETATS-UNIS, 2000.
- 545 Chambers, J. Q., Fisher, J. I., Zeng, H., Chapman, E. L., Baker, D. B., and Hurtt, G. C.: Hurricane
546 Katrina's Carbon Footprint on U.S. Gulf Coast Forests, *Science*, 318, 1107-
547 10.1126/science.1148913, 2007.
- 548 Clark, K. L., Gholz, H. L., Moncrieff, J. B., Cropley, F., and Loescher, H. W.: Environmental Controls
549 over Net Exchanges of Carbon Dioxide from Contrasting Florida Ecosystems, *Ecological*
550 *Applications*, 9, 936-948, 1999.
- 551 Clark, K. L., Gholz, H. L., and Castro, M. S.: Carbon dynamics along a chronosequence of slash pine
552 plantations in north florida, *Ecological Applications*, 14, 1154-1171, doi:10.1890/02-5391,
553 2004.
- 554 Cook, B. D., Davis, K. J., Wang, W., Desai, A., Berger, B. W., Teclaw, R. M., Martin, J. G., Bolstad, P. V.,
555 Bakwin, P. S., Yi, C., and Heilman, W.: Carbon exchange and venting anomalies in an upland
556 deciduous forest in northern Wisconsin, USA, *Agricultural and Forest Meteorology*, 126,
557 271-295, 2004.
- 558 Coops, N. C., Waring, R. H., and Landsberg, J. J.: Assessing forest productivity in Australia and New
559 Zealand using a physiologically-based model driven with averaged monthly weather data and
560 satellite-derived estimates of canopy photosynthetic capacity, *Forest Ecology and Management*,
561 104, 113-127, 1998.
- 562 Coulter, R. L., Pekour, M. S., Cook, D. R., Klazura, G. E., Martin, T. J., and Lucas, J. D.: Surface energy
563 and carbon dioxide fluxes above different vegetation types within ABLE, *Agricultural and*
564 *Forest Meteorology*, 136, 147-158, 2006.
- 565 Deng, F., Chen, J. M., Ishizawa, M., Yuen, C.-W., Mo, G., Higuchi, K., Chan, D., and Maksyutov, S.:

566 Global monthly CO₂ flux inversion with a focus over North America, *Tellus B*, 59, 179-190,
567 2007.

568 Falk, M., Wharton, S., Schroeder, M., Ustin, S., and U, K. T. P.: Flux partitioning in an old-growth
569 forest: seasonal and interannual dynamics, *Tree Physiol*, 28, 509-520,
570 10.1093/treephys/28.4.509, 2008.

571 Fan, S., Gloor, M., Mahlman, J., Pacala, S., Sarmiento, J., Takahashi, T., and Tans, P.: A Large
572 Terrestrial Carbon Sink in North America Implied by Atmospheric and Oceanic Carbon
573 Dioxide Data and Models, *Science*, 282, 442-446, 10.1126/science.282.5388.442, 1998.

574 Field, C. B., Randerson, J. T., and Malmström, C. M.: Global net primary production: Combining
575 ecology and remote sensing, *Remote Sensing of Environment*, 51, 74-88, 1995.

576 Goward, S. N., and Huemmrich, K. F.: Vegetation canopy PAR absorptance and the normalized
577 difference vegetation index: An assessment using the SAIL model, *Remote Sensing of
578 Environment*, 39, 119-140, 1992.

579 Green, E. J., MacFarlane, D. W., Valentine, H. T., and Strawderman, W. E.: Assessing Uncertainty in a
580 Stand Growth Model by Bayesian Synthesis, *Forest Science*, 45, 528-538, 1999.

581 Griffis, T. J., Sargent, S. D., Baker, J. M., Lee, X., Tanner, B. D., Greene, J., Swiatek, E., and Billmark,
582 K.: Direct measurement of biosphere-atmosphere isotopic CO₂ exchange using the eddy
583 covariance technique, *J. Geophys. Res.*, 113, D08304, 10.1029/2007jd009297, 2008.

584 Guenther, B., Xiong, X., Salomonson, V. V., Barnes, W. L., and Young, J.: On-orbit performance of the
585 Earth Observing System Moderate Resolution Imaging Spectroradiometer; first year of data,
586 *Remote Sensing of Environment*, 83, 16-30, 2002.

587 Gurney, K. R., Law, R. M., Denning, A. S., Rayner, P. J., Baker, D., Bousquet, P., Bruhwiler, L., Chen,
588 Y.-H., Ciais, P., Fan, S., Fung, I. Y., Gloor, M., Heimann, M., Higuchi, K., John, J., Maki, T.,
589 Maksyutov, S., Masarie, K., Peylin, P., Prather, M., Pak, B. C., Randerson, J., Sarmiento, J.,
590 Taguchi, S., Takahashi, T., and Yuen, C.-W.: Towards robust regional estimates of CO₂ sources
591 and sinks using atmospheric transport models, *Nature*, 415, 626-630,
592 http://www.nature.com/nature/journal/v415/n6872/supinfo/415626a_S1.html, last access:
593 June 2009. 2002.

594 Hazarika, M. K., Yasuoka, Y., Ito, A., and Dye, D.: Estimation of net primary productivity by
595 integrating remote sensing data with an ecosystem model, *Remote Sensing of Environment*, 94,
596 298-310, 2005.

597 Hollinger, D. Y., Goltz, S. M., Davidson, E. A., Lee, J. T., Tu, K., and Valentine, H. T.: Seasonal patterns
598 and environmental control of carbon dioxide and water vapour exchange in an ecotonal boreal
599 forest, *Global Change Biology*, 5, 891-902, 1999.

600 Hollinger, D. Y., Aber, J., Dail, B., Davidson, E. A., Goltz, S. M., Hughes, H., Leclerc, M. Y., Lee, J. T.,
601 Richardson, A. D., Rodrigues, C., Scott, N. A., Achuatavariet, D., and Walsh, J.: Spatial and
602 temporal variability in forest-atmosphere CO₂ exchange, *Global Change Biology*,
603 10, 1689-1706, 2004.

604 Hollinger, S. E., Bernacchi, C. J., and Meyers, T. P.: Carbon budget of mature no-till ecosystem in North
605 Central Region of the United States, *Agricultural and Forest Meteorology*, 130, 59-69, 2005.

606 Houghton, R. A., Hackler, J. L., and Lawrence, K. T.: The U.S. Carbon Budget: Contributions from
607 Land-Use Change, *Science*, 285, 574-578, 10.1126/science.285.5427.574, 1999.

608 Houghton, R. A., and Hackler, J. L.: Changes in Terrestrial Carbon Storage in the United States. 1: The
609 Roles of Agriculture and Forestry, *Global Ecology and Biogeography*, 9, 125-144, 2000.

- 610 Houghton, R. A., Hackler, J. L., and Lawrence, K. T.: Changes in Terrestrial Carbon Storage in the
611 United States. 2: The Role of Fire and Fire Management, *Global Ecology and Biogeography*, 9,
612 145-170, 2000.
- 613 Huete, A., Liu, H. Q., Batchily, K., and van Leeuwen, W.: A comparison of vegetation indices over a
614 global set of TM images for EOS-MODIS, *Remote Sensing of Environment*, 59, 440-451,
615 1997.
- 616 Huete, A., Didan, K., Miura, T., Rodriguez, E. P., Gao, X., and Ferreira, L. G.: Overview of the
617 radiometric and biophysical performance of the MODIS vegetation indices, *Remote Sensing of*
618 *Environment*, 83, 195-213, 2002.
- 619 Iman, R. L., and Helton, J. C.: An Investigation of Uncertainty and Sensitivity Analysis Techniques for
620 Computer Models, *Risk Analysis*, 8, 71-90, 1988.
- 621 IPCC: Climate Change 2001: Synthesis Report. A Contribution of Working Groups I, II, and III to the
622 Third Assessment Report of the Intergovernmental Panel on Climate Change, edited by:
623 Watson, R. T., and the Core Writing Team, Cambridge University Press, Cambridge, United
624 Kingdom and New York, NY, 2001.
- 625 Justice, C. O., Townshend, J. R. G., Vermote, E. F., Masuoka, E., Wolfe, R. E., Saleous, N., Roy, D. P.,
626 and Morisette, J. T.: An overview of MODIS Land data processing and product status, *Remote*
627 *Sensing of Environment*, 83, 3-15, 2002.
- 628 Kistler, R., Collins, W., Saha, S., White, G., Woollen, J., Kalnay, E., Chelliah, M., Ebisuzaki, W.,
629 Kanamitsu, M., Kousky, V., van den Dool, H., Jenne, R., and Fiorino, M.: The NCEP-NCAR
630 50-Year Reanalysis: Monthly Means CD-ROM and Documentation, *Bulletin of the American*
631 *Meteorological Society*, 82, 247-267,
632 doi:10.1175/1520-0477(2001)082<0247:TNNYRM>2.3.CO2, 2001.
- 633 Law, B., Turner, D., Campbell, J., Lefsky, M., Guzy, M., Sun, O., Tuyl, S., and Cohen, W.: Carbon
634 fluxes across regions: observational constraints at multiple scales, in: *Scaling and Uncertainty*
635 *Analysis in Ecology: Methods and Applications*, edited by: Wu, J., Jones, K. B., Li, H., and
636 Loucks, O. L., Columbia University Press, New York, 167-190, 2006.
- 637 Li, Z., Yu, G., Xiao, X., Li, Y., Zhao, X., Ren, C., Zhang, L., and Fu, Y.: Modeling gross primary
638 production of alpine ecosystems in the Tibetan Plateau using MODIS images and climate data,
639 *Remote Sensing of Environment*, 107, 510-519, 2007.
- 640 Lipson, D. A., Wilson, R. F., and Oechel, W. C.: Effects of Elevated Atmospheric CO₂ on Soil
641 Microbial Biomass, Activity, and Diversity in a Chaparral Ecosystem, *Appl. Environ.*
642 *Microbiol.*, 71, 8573-8580, 10.1128/aem.71.12.8573-8580.2005, 2005.
- 643 Lu, X., and Zhuang, Q.: Evaluating climate impacts on carbon balance of the terrestrial ecosystems in
644 the Midwest of the United States with a process-based ecosystem model, *Mitigation and*
645 *Adaptation Strategies for Global Change*, 2010.
- 646 Ma, S., Baldocchi, D. D., Xu, L., and Hehn, T.: Inter-annual variability in carbon dioxide exchange of
647 an oak/grass savanna and open grassland in California, *Agricultural and Forest Meteorology*,
648 147, 157-171, 2007.
- 649 McGuire, A. D., Melillo, J. M., Joyce, L. A., Kicklighter, D. W., Grace, A. L., Moore, B., III, and
650 Vorosmarty, C. J.: Interactions Between Carbon and Nitrogen Dynamics in Estimating Net
651 Primary Productivity For Potential Vegetation in North America, *Global Biogeochem. Cycles*,
652 6, 10.1029/92gb00219, 1992.
- 653 McGuire, A. D., Sitch, S., Clein, J. S., Dargaville, R., Esser, G., Foley, J., Heimann, M., Joos, F., Kaplan,

654 J., Kicklighter, D. W., Meier, R. A., Melillo, J. M., Moore, B., III, Prentice, I. C., Ramankutty,
655 N., Reichenau, T., Schloss, A., Tian, H., Williams, L. J., and Wittenberg, U.: Carbon Balance of
656 the Terrestrial Biosphere in the Twentieth Century: Analyses of CO₂, Climate and Land Use
657 Effects With Four Process-Based Ecosystem Models, *Global Biogeochem. Cycles*, 15, 183-206,
658 10.1029/2000gb001298, 2001.

659 McMurtrie, R. E., Gower, S. T., and Ryan, M. G.: Forest Productivity: Explaining Its Decline with Stand
660 Age, *Bulletin of the Ecological Society of America*, 76, 152-154, 1995.

661 Melillo, J. M., McGuire, A. D., Kicklighter, D. W., Moore, B., Vorosmarty, C. J., and Schloss, A. L.:
662 Global climate change and terrestrial net primary production, *Nature*, 363, 234-240, 1993.

663 Moffat, A. M., Papale, D., Reichstein, M., Hollinger, D. Y., Richardson, A. D., Barr, A. G., Beckstein,
664 C., Braswell, B. H., Churkina, G., Desai, A. R., Falge, E., Gove, J. H., Heimann, M., Hui, D.,
665 Jarvis, A. J., Kattge, J., Noormets, A., and Stauch, V. J.: Comprehensive comparison of
666 gap-filling techniques for eddy covariance net carbon fluxes, *Agricultural and Forest
667 Meteorology*, 147, 209-232, 2007.

668 Monson, R. K., Turnipseed, A. A., Sparks, J. P., Harley, P. C., Scott-Denton, L. E., Sparks, K., and
669 Huxman, T. E.: Carbon sequestration in a high-elevation, subalpine forest, *Global Change
670 Biology*, 8, 459-478, 2002.

671 Myneni, R. B., Hoffman, S., Knyazikhin, Y., Privette, J. L., Glassy, J., Tian, Y., Wang, Y., Song, X.,
672 Zhang, Y., Smith, G. R., Lotsch, A., Friedl, M., Morisette, J. T., Votava, P., Nemani, R. R., and
673 Running, S. W.: Global products of vegetation leaf area and fraction absorbed PAR from year
674 one of MODIS data, *Remote Sensing of Environment*, 83, 214-231, 2002.

675 Pacala, S. W., Hurtt, G. C., Baker, D., Peylin, P., Houghton, R. A., Birdsey, R. A., Heath, L., Sundquist,
676 E. T., Stallard, R. F., Ciais, P., Moorcroft, P., Caspersen, J. P., Shevliakova, E., Moore, B.,
677 Kohlmaier, G., Holland, E., Gloor, M., Harmon, M. E., Fan, S.-M., Sarmiento, J. L., Goodale, C.
678 L., Schimel, D., and Field, C. B.: Consistent Land- and Atmosphere-Based U.S. Carbon Sink
679 Estimates, *Science*, 292, 2316-2320, 10.1126/science.1057320, 2001.

680 Papale, D., and Valentini, R.: A new assessment of European forests carbon exchanges by eddy fluxes
681 and artificial neural network spatialization, *Global Change Biology*, 9, 525-535, 2003.

682 Pinter, P. J., Jackson, R. D., Idso, S. B., and Reginato, R. J.: Diurnal Patterns of Wheat Spectral
683 Reflectances, *Geoscience and Remote Sensing, IEEE Transactions on*, GE-21, 156-163, 1983.

684 Pinter, P. J., Jackson, R. D., Ezra, C. E., and Gausman, H. W.: Sun-angle and canopy-architecture effects
685 on the spectral reflectance of six wheat cultivars, *International Journal of Remote Sensing*, 6,
686 1813 - 1825, 1985.

687 Potter, C., Klooster, S., Myneni, R., Genovese, V., Tan, P.-N., and Kumar, V.: Continental-scale
688 comparisons of terrestrial carbon sinks estimated from satellite data and ecosystem modeling
689 1982-1998, *Global and Planetary Change*, 39, 201-213, 2003.

690 Potter, C., Klooster, S., Huete, A., and Genovese, V.: Terrestrial Carbon Sinks for the United States
691 Predicted from MODIS Satellite Data and Ecosystem Modeling, *Earth Interactions*, 11, 1-21,
692 doi:10.1175/EI228.1, 2007.

693 Potter, C. S., Randerson, J. T., Field, C. B., Matson, P. A., Vitousek, P. M., Mooney, H. A., and Klooster,
694 S. A.: Terrestrial Ecosystem Production: a Process Model Based on Global Satellite and
695 Surface Data, *Global Biogeochem. Cycles*, 7, 10.1029/93gb02725, 1993.

696 Prince, S. D. and Goward, S. N.: Global primary production: A remote sensing approach. *Journal of
697 Biogeography*, 22, 815-835, 1995.

698 Rahman, A. F., Sims, D. A., Cordova, V. D., and El-Masri, B. Z.: Potential of MODIS EVI and surface
699 temperature for directly estimating per-pixel ecosystem C fluxes, *Geophys. Res. Lett.*, 32,
700 L19404, 10.1029/2005gl024127, 2005.

701 Raich, J. W., Rastetter, E. B., Melillo, J. M., Kicklighter, D. W., Steudler, P. A., Peterson, B. J., Grace, A.
702 L., Iii, B. M., and Vörösmarty, C. J.: Potential Net Primary Productivity in South America:
703 Application of a Global Model, *Ecological Applications*, 1, 399-429, 1991.

704 Ratana, P., Huete, A. R., Yuan, Y., and Jacobson, A.: Interrelationship among among MODIS vegetation
705 products across an Amazon Eco-climatic gradient, *Geoscience and Remote Sensing*
706 *Symposium*, 2005. IGARSS '05. Proceedings. 2005 IEEE International, 2005, 3009-3012,
707 25-29 July 2005, Seoul, Korea, 2005.

708 Reichstein, M., Subke, J.-A., Angeli, A. C., and Tenhunen, J. D.: Does the temperature sensitivity of
709 decomposition of soil organic matter depend upon water content, soil horizon, or incubation
710 time?, *Global Change Biology*, 11, 1754-1767, 2005.

711 Richardson, A. D., Mahecha, M. D., Falge, E., Kattge, J., Moffat, A. M., Papale, D., Reichstein, M.,
712 Stauch, V. J., Braswell, B. H., Churkina, G., Kruijt, B., and Hollinger, D. Y.: Statistical
713 properties of random CO₂ flux measurement uncertainty inferred from model residuals,
714 *Agricultural and Forest Meteorology*, 148, 38-50, 2008.

715 Running, S., Nemani, R., Heinsch, F., Zhao, M., Reeves, M., and Hashimoto, H.: A continuous
716 satellite-derived measure of global terrestrial primary production, *BioScience*, 54, 547 - 560,
717 2004.

718 Running, S. W., Nemani, R., Glassy, J. M., & Thornton, P.: MODIS Daily photosynthesis (PSN) and
719 annual net primary production (NPP) product (MOD17), Algorithm Theoretical Basis
720 Document, Version 3.0, April 29, 1999.

721 Running, S. W., Thornton, P. E., Nemani, R., & Glassy, J. M.: Global terrestrial gross and net primary
722 productivity from the Earth Observing System. In O. E. Sala, R. B. Jackson, H. A. Mooney, and
723 R. W. Howarth (Eds.), *Methods in ecosystem science* (pp. 44 – 57). New York: Springer. 2000.

724 Running, S. W., and Hunt, E. R., Jr.: Generalization of a forest ecosystem process model for other
725 biomes, BIOME-BGC, and an application for global-scale models., in: *Scaling Physiological*
726 *Processes: Leaf to Globe*, edited by: Field, J. R. E. a. C., Academic Press, San Diego, CA,
727 141-158, 1993.

728 Santaren, D., Peylin, P., Viovy, N., and Ciais, P.: Optimizing a process-based ecosystem model with
729 eddy-covariance flux measurements: A pine forest in southern France, *Global Biogeochem.*
730 *Cycles*, 21, 10.1029/2006gb002834, 2007.

731 Schimel, D., Melillo, J., Tian, H., McGuire, A. D., Kicklighter, D., Kittel, T., Rosenbloom, N., Running,
732 S., Thornton, P., Ojima, D., Parton, W., Kelly, R., Sykes, M., Neilson, R., and Rizzo, B.:
733 Contribution of Increasing CO₂ and Climate to Carbon Storage by Ecosystems in the United
734 States, *Science*, 287, 2004-2006, 10.1126/science.287.5460.2004, 2000.

735 Schmid, H. P., Grimmond, C. S. B., Cropley, F., Offerle, B., and Su, H.-B.: Measurements of CO₂ and
736 energy fluxes over a mixed hardwood forest in the mid-western United States, *Agricultural and*
737 *Forest Meteorology*, 103, 357-374, 2000.

738 Schmid, H. P.: Footprint modeling for vegetation atmosphere exchange studies: a review and
739 perspective, *Agricultural and Forest Meteorology*, 113, 159-183, 2002.

740 Scott, R. L., Cable, W. L., and Hultine, K. R.: The ecohydrologic significance of hydraulic
741 redistribution in a semiarid savanna, *Water Resour. Res.*, 44, W02440, 10.1029/2007wr006149,

742 2008.

743 Scott, R. L., Hamerlynck, E. P., Jenerette, G. D., Moran, M. S., and Barron-Gafford, G. A.: Carbon
744 dioxide exchange in a semidesert grassland through drought-induced vegetation change, *J.*
745 *Geophys. Res.*, 115, G03026, 10.1029/2010jg001348, 2010.

746 Seaquist, J. W., Olsson, L., and Ardö, J.: A remote sensing-based primary production model for
747 grassland biomes, *Ecological Modelling*, 169, 131-155, 2003.

748 Sims, D. A., Rahman, A. F., Cordova, V. D., El-Masri, B. Z., Baldocchi, D. D., Flanagan, L. B.,
749 Goldstein, A. H., Hollinger, D. Y., Misson, L., Monson, R. K., Oechel, W. C., Schmid, H. P.,
750 Wofsy, S. C., and Xu, L.: On the use of MODIS EVI to assess gross primary productivity of
751 North American ecosystems, *J. Geophys. Res.*, 111, G04015, 10.1029/2006jg000162, 2006.

752 Sims, D. A., Rahman, A. F., Cordova, V. D., El-Masri, B. Z., Baldocchi, D. D., Bolstad, P. V., Flanagan,
753 L. B., Goldstein, A. H., Hollinger, D. Y., Misson, L., Monson, R. K., Oechel, W. C., Schmid, H.
754 P., Wofsy, S. C., and Xu, L.: A new model of gross primary productivity for North American
755 ecosystems based solely on the enhanced vegetation index and land surface temperature from
756 MODIS, *Remote Sensing of Environment*, 112, 1633-1646, 2008.

757 Skare, Ø., Bølviken, E., and Holden, L.: Improved Sampling-Importance Resampling and Reduced
758 Bias Importance Sampling, *Scandinavian Journal of Statistics*, 30, 719-737, 2003.

759 Suyker, A. E., Verma, S. B., Burba, G. G., and Arkebauer, T. J.: Gross primary production and ecosystem
760 respiration of irrigated maize and irrigated soybean during a growing season, *Agricultural and*
761 *Forest Meteorology*, 131, 180-190, 2005.

762 Tang, J., and Zhuang, Q.: Equifinality in parameterization of process-based biogeochemistry models: A
763 significant uncertainty source to the estimation of regional carbon dynamics, *J. Geophys. Res.*,
764 113, 10.1029/2008jg000757, 2008.

765 Tang, J., and Zhuang, Q.: A global sensitivity analysis and Bayesian inference framework for improving
766 the parameter estimation and prediction of a process-based Terrestrial Ecosystem Model, *J.*
767 *Geophys. Res.*, 114, 10.1029/2009jd011724, 2009.

768 Turner, D. P., Koerper, G. J., Harmon, M. E., and Lee, J. J.: A Carbon Budget for Forests of the
769 Conterminous United States, *Ecological Applications*, 5, 421-436, doi:10.2307/1942033, 1995.

770 Urbanski, S., Barford, C., Wofsy, S., Kucharik, C., Pyle, E., Budney, J., McKain, K., Fitzjarrald, D.,
771 Czikowsky, M., and Munger, J. W.: Factors controlling CO₂ exchange on timescales from
772 hourly to decadal at Harvard Forest, *J. Geophys. Res.*, 112, G02020, 10.1029/2006jg000293,
773 2007.

774 Wang, Y.-P., Leuning, R., Cleugh, H. A., and Coppin, P. A.: Parameter estimation in surface exchange
775 models using nonlinear inversion: how many parameters can we estimate and which
776 measurements are most useful?, *Global Change Biology*, 7, 495-510, 2001.

777 Wang, Y.-p., BALDOCCHI, D., LEUNING, R., FALGE, E., and VESALA, T.: Estimating parameters
778 in a land-surface model by applying nonlinear inversion to eddy covariance flux measurements
779 from eight FLUXNET sites, *Global Change Biology*, 13, 652-670, 2007.

780 Waring, R. H., Milner, K. S., Jolly, W. M., Phillips, L., and McWethy, D.: Assessment of site index and
781 forest growth capacity across the Pacific and Inland Northwest U.S.A. with a MODIS
782 satellite-derived vegetation index, *Forest Ecology and Management*, 228, 285-291, 2006.

783 Williams, M., Schwarz, P. A., Law, B. E., Irvine, J., and Kurpius, M. R.: An improved analysis of forest
784 carbon dynamics using data assimilation, *Global Change Biology*, 11, 89-105, 2005.

785 Wofsy, S. C., Goulden, M. L., Munger, J. W., Fan, S.-M., Bakwin, P. S., Daube, B. C., Bassow, S. L.,

786 and Bazzaz, F. A.: Net Exchange of CO₂ in a Mid-Latitude Forest, *Science*, 260, 1314-1317,
787 10.1126/science.260.5112.1314, 1993.

788 Wolfe, R. E., Nishihama, M., Fleig, A. J., Kuyper, J. A., Roy, D. P., Storey, J. C., and Patt, F. S.:
789 Achieving sub-pixel geolocation accuracy in support of MODIS land science, *Remote Sensing*
790 *of Environment*, 83, 31-49, 2002.

791 Xiao, J., Zhuang, Q., Baldocchi, D. D., Law, B. E., Richardson, A. D., Chen, J., Oren, R., Starr, G.,
792 Noormets, A., Ma, S., Verma, S. B., Wharton, S., Wofsy, S. C., Bolstad, P. V., Burns, S. P., Cook,
793 D. R., Curtis, P. S., Drake, B. G., Falk, M., Fischer, M. L., Foster, D. R., Gu, L., Hadley, J. L.,
794 Hollinger, D. Y., Katul, G. G., Litvak, M., Martin, T. A., Matamala, R., McNulty, S., Meyers, T.
795 P., Monson, R. K., Munger, J. W., Oechel, W. C., Paw U, K. T., Schmid, H. P., Scott, R. L., Sun,
796 G., Suyker, A. E., and Torn, M. S.: Estimation of net ecosystem carbon exchange for the
797 conterminous United States by combining MODIS and AmeriFlux data, *Agricultural and*
798 *Forest Meteorology*, 148, 1827-1847, 2008.

799 Xiao, J., Zhuang, Q., Law, B. E., Chen, J., Baldocchi, D. D., Cook, D. R., Oren, R., Richardson, A. D.,
800 Wharton, S., Ma, S., Martin, T. A., Verma, S. B., Suyker, A. E., Scott, R. L., Monson, R. K.,
801 Litvak, M., Hollinger, D. Y., Sun, G., Davis, K. J., Bolstad, P. V., Burns, S. P., Curtis, P. S.,
802 Drake, B. G., Falk, M., Fischer, M. L., Foster, D. R., Gu, L., Hadley, J. L., Katul, G. G.,
803 Matamala, R., McNulty, S., Meyers, T. P., Munger, J. W., Noormets, A., Oechel, W. C., Paw U,
804 K. T., Schmid, H. P., Starr, G., Torn, M. S., and Wofsy, S. C.: A continuous measure of gross
805 primary production for the conterminous United States derived from MODIS and AmeriFlux
806 data, *Remote Sensing of Environment*, 114, 576-591, 2010.

807 Xiao, J., Zhuang, Q., Law, B. E., Baldocchi, D. D., Chen, J., Richardson, A. D., Melillo, J. M., Davis, K.
808 J., Hollinger, D. Y., Wharton, S., Oren, R., Noormets, A., Fischer, M. L., Verma, S. B., Cook, D.
809 R., Sun, G., McNulty, S., Wofsy, S. C., Bolstad, P. V., Burns, S. P., Curtis, P. S., Drake, B. G.,
810 Falk, M., Foster, D. R., Gu, L., Hadley, J. L., Katul, G. G., Litvak, M., Ma, S., Martin, T. A.,
811 Matamala, R., Meyers, T. P., Monson, R. K., Munger, J. W., Oechel, W. C., Paw, U. K. T.,
812 Schmid, H. P., Scott, R. L., Starr, G., Suyker, A. E., and Torn, M. S.: Assessing net ecosystem
813 carbon exchange of U.S. terrestrial ecosystems by integrating eddy covariance flux
814 measurements and satellite observations, *Agricultural and Forest Meteorology*, 151, 60-69,
815 2011.

816 Xiao, X., Hollinger, D., Aber, J., Goltz, M., Davidson, E. A., Zhang, Q., and Moore, B.: Satellite-based
817 modeling of gross primary production in an evergreen needleleaf forest, *Remote Sensing of*
818 *Environment*, 89, 519-534, 2004.

819 Xu, L., and Baldocchi, D. D.: Seasonal variation in carbon dioxide exchange over a Mediterranean
820 annual grassland in California, *Agricultural and Forest Meteorology*, 123, 79-96, 2004.

821 Yan, H., Fu, Y., Xiao, X., Huang, H. Q., He, H., and Ediger, L.: Modeling gross primary productivity for
822 winter wheat-maize double cropping system using MODIS time series and CO₂ eddy flux
823 tower data, *Agriculture, Ecosystems & Environment*, 129, 391-400, 2009.

824 Yang, F., Ichii, K., White, M. A., Hashimoto, H., Michaelis, A. R., Votava, P., Zhu, A. X., Huete, A.,
825 Running, S. W., and Nemani, R. R.: Developing a continental-scale measure of gross primary
826 production by combining MODIS and AmeriFlux data through Support Vector Machine
827 approach, *Remote Sensing of Environment*, 110, 109-122, 2007.

828 Zhao, M., Heinsch, F. A., Nemani, R. R., and Running, S. W.: Improvements of the MODIS terrestrial
829 gross and net primary production global data set, *Remote Sensing of Environment*, 95, 164-176,

830 2005.

831 Zhao, M., Running, S. W., and Nemani, R. R.: Sensitivity of Moderate Resolution Imaging
832 Spectroradiometer (MODIS) terrestrial primary production to the accuracy of meteorological
833 reanalyses, *J. Geophys. Res.*, 111, G01002, 10.1029/2004jg000004, 2006.

834 Zhao, M., and Running, S. W.: Remote Sensing of Terrestrial Primary Production and Carbon Cycle, in,
835 423-444, 2008.

836 Zhuang, Q., Romanovsky, V. E., and McGuire, A. D.: Incorporation of a permafrost model into a
837 large-scale ecosystem model: Evaluation of temporal and spatial scaling issues in simulating
838 soil thermal dynamics, *J. Geophys. Res.*, 106, 10.1029/2001jd900151, 2001.

839 Zhuang, Q., McGuire, A. D., O'Neill, K. P., Harden, J. W., Romanovsky, V. E., and Yarie, J.: Modeling
840 soil thermal and carbon dynamics of a fire chronosequence in interior Alaska, *J. Geophys. Res.*,
841 107, 10.1029/2001jd001244, 2002.

842 Zhuang, Q., McGUIRE, A. D., MELILLO, J. M., CLEIN, J. S., DARGAVILLE, R. J., KICKLIGHTER,
843 D. W., MYNENI, R. B., DONG, J., ROMANOVSKY, V. E., HARDEN, J., and HOBBIE, J. E.:
844 Carbon cycling in extratropical terrestrial ecosystems of the Northern Hemisphere during the
845 20th century: a modeling analysis of the influences of soil thermal dynamics, *Tellus B*, 55,
846 751-776, 2003.

847 Zhuang, Q., Melillo, J. M., Kicklighter, D. W., Prinn, R. G., McGuire, A. D., Steudler, P. A., Felzer, B. S.,
848 and Hu, S.: Methane fluxes between terrestrial ecosystems and the atmosphere at northern high
849 latitudes during the past century: A retrospective analysis with a process-based
850 biogeochemistry model, *Global Biogeochem. Cycles*, 18, 10.1029/2004gb002239, 2004.

851

852

853

854 **Figure Captions**

855 Figure 1. Land cover map of the conterminous U.S. ($0.05^\circ \times 0.05^\circ$) used in regional simulations. The
856 map was re-classified based on MODIS product Land Cover Types Yearly L3 Global 0.05 Deg CMG
857 (MOD12C1). Red pins indicate the location of the AmeriFlux sites used in this study.

858
859 Figure 2. Comparison of seasonal variations of the observed GPP and NEP with SAT-TEM and TEM
860 predicted ones at the six parameterization sites. Dashed lines are the observations while circles and
861 crosses are the predictions with SAT-TEM and TEM, respectively. The error bars indicates the standard
862 deviation of the results by ensemble SAT-TEM simulations with 50 sets of posterior parameters. Data
863 during the periods before the vertical dotted lines are used for parameterization while the remaining are
864 verification results at: (a) Howland Forest West Tower site; (b) Harvard Forest site (c) Vaira Ranch site;
865 (d) Sky Oaks New site; (e) Tonzi Ranch site; (f) Bondville site.

866
867 Figure 3. Comparison of seasonal variations of the observed GPP and NEP with SAT-TEM and TEM
868 predictions at the ten additional AmeriFlux sites. Dashed lines are the observed values while circles and
869 crosses are the predictions with SAT-TEM and TEM, respectively. The error bars indicates the standard
870 deviation of the results by ensemble SAT-TEM simulations with 50 sets of posterior parameters: (a)
871 Niwot Ridge site; (b) Wind River Crane site (c) Morgan Monroe State Forest site; (d) Willow Creek site;
872 (e) Kendall Grassland site; (f) Walnut River site; (g) Sky Oaks Old site; (h) Santa Rita Mesquite
873 Savanna site; (i) Rosemount G21 Conventional Management Corn Soybean Rotation site; (j) Mead
874 Irrigated Rotation site.

875
876 Figure 4. Scatterplots of the observed GPP and NEP versus SAT-TEM and TEM predictions at the
877 selected AmeriFlux sites. Black dashed lines show a 1:1 relationship. Circles and crosses, red and blue
878 regression lines are SAT-TEM and TEM simulated values, respectively. The error bars indicates the
879 standard deviation of the results by ensemble SAT-TEM simulations with 50 sets of posterior
880 parameters. (a) and (b) are the predicted GPP and NEP versus observed values, respectively.

881
882 Figure 5. Annual average SAT-TEM estimated NEP across the conterminous United States for each year
883 in 2000-2005. Positive values represent carbon sink while negative values represent carbon source.
884 Units are $\text{g C m}^{-2} \text{ yr}^{-1}$.

885
886 Figure 6. Comparison between NEP, EVI, and LSWI across the conterminous United States over the
887 period of 2000-2005: (a) Cumulative monthly NEP estimated by SAT-TEM. (b) Monthly averaged
888 regional EVI,. (c) Monthly averaged regional LSWI.

889
890 Figure 7. Average annual carbon fluxes ($\text{g C m}^{-2} \text{ yr}^{-1}$) (left) and the relative standard deviations (right) of
891 the conterminous United States over the period 2000-2005: (a) GPP; (b) NPP; (c) NEP. The relative
892 standard deviations are calculated by dividing standard deviations by the average values of the regional
893 results of the 50 sets of simulations.

894
895 Figure 8. Impacts of Hurricane Katrina on two-month-average EVI and estimated GPP. Units for GPP
896 are $\text{g C m}^{-2} \text{ month}^{-1}$.

897

898 Table 1. Characteristics of AmeriFlux sites used in this study.

<i>Site Name</i>	<i>Latitude (°)</i>	<i>Longitude (°)</i>	<i>Vegetation Type</i>	<i>Years</i>	<i>References</i>
Howland Forest West Tower (ME, USA)*	45.2091	-68.7470	Evergreen Forest	2000-2004	Hollinger et al., (1999, 2004)
Harvard Forest (MA, USA)*	42.5378	-72.1715	Deciduous Forest	2000-2006	Urbanski et al., (2007) Xu and
Vaira Ranch (CA, USA)*	38.4061	-120.9507	Grassland	2002-2007	Baldocchi, (2004)
Sky Oaks New (CA, USA)*	33.3844	-116.6403	Shrubland	2004-2006	Lipson et al., (2005)
Tonzi Ranch (CA, USA)*	38.4316	-120.9660	Savannas	2002-2007	Ma et al., (2007)
Bondville (IL, USA)*	40.0062	-88.2904	Cropland	2001-2006	Hollinger et al., (2005)
Niwot Ridge (CO, USA)	40.0329	-105.5464	Evergreen Forest	2000-2005	Monson et al., (2002)
Wind River Crane site (WA, USA)	45.8205	-121.9519	Evergreen Forest	2000-2002	Falk et al., (2008)
Morgan Monroe State Forest (IN, USA)	39.3232	-86.4131	Deciduous Forest	2001-2006	Schmid et al., (2000)
Willow Creek (WI, USA)	45.8059	-90.0799	Deciduous Forest	2000-2003	Cook et al., (2004)
Kendall Grassland (AZ, USA)	31.7365	-109.9419	Grassland	2005-2007	Scott et al., (2010)
Walnut River (KS, USA)	37.5208	-96.8550	Grassland	2002-2003	Coulter et al., (2006)
Sky Oaks Old (CA, USA)	33.3739	-116.6229	Shrubland	2004-2006	Lipson et al., (2005)
Santa Rita Mesquite Savanna (AZ, USA)	31.8214	-110.8661	Savannas	2004-2006	Scott et al., (2008)
Rosemount G21 Conventional Management Corn Soybean Rotation (MN, USA)	44.7143	-93.0898	Cropland	2004-2006	Griffis et al., (2008)
Mead Irrigated Rotation (NE, USA)	41.1649	-96.4701	Cropland	2002-2005	Suyker et al., (2005)

899 * Sites for parameterization.

900 Table 2. Reclassification of MODIS land covers to TEM vegetation types

<i>MODIS Land Cover Types(IGBP)</i>	<i>Vegetation Community Type in SAT-TEM</i>
Evergreen needleleaf forest	Evergreen Forest
Evergreen broadleaf forest	Evergreen Forest
Deciduous needleleaf forest	Deciduous Forest
Deciduous broadleaf forest	Deciduous Forest
Mixed forest	50% Evergreen Forest, 50% Deciduous Forest
Closed shrubland	Shrubland
Open shrubland	Shrubland
Woody savannas	Savannas
Savannas	Savannas
Grassland	Grassland
Permanent Wetland	Grassland
Cropland	Cropland
Cropland and natural vegetation mosaic	Cropland

901

902 Table 3. Key TEM Parameters

903

Parameter	Definition	Unit	Prior Range
k_i	Half saturation constant for PAR used by plants	$\mu\text{L L}^{-1}$	[100.0, 500.0]
k_c	Half saturation constant for CO ₂ -C uptake by plants	$\mu\text{L L}^{-1}$	[100.0, 400.0]
<i>RAQ10A0</i>	Leading coefficient of the Q10 model for plant respiration	None	[1.0, 3.0]
<i>RAQ10A1</i>	1 st order coefficient of the Q10 model for plant respiration	$^{\circ}\text{C}^{-1}$	[-0.1, 0.1]
<i>RAQ10A2</i>	2 nd order coefficient of the Q10 model for plant respiration	$^{\circ}\text{C}^{-2}$	[0, 0.005]
<i>RAQ10A3</i>	3 rd order coefficient of the Q10 model for plant respiration	$^{\circ}\text{C}^{-3}$	[0.0001, 0.001]
<i>RHQ10</i>	Change in heterotrophic respiration rate due to 10 $^{\circ}\text{C}$ temperature increase	None	[1.0, 3.0]
<i>MOISTOPT</i>	Optimum soil moisture content for heterotrophic respiration	%	[0.2, 0.8]
C_{max}	Maximum rate of photosynthesis C	$\text{g C m}^{-2} \text{ month}^{-1}$	[500.0, 3000.0]
K_r	Logarithm of plant respiration rate at 0 $^{\circ}\text{C}$	$\text{g g}^{-1} \text{ month}^{-1}$	[-9.5, -0.2]
K_d	Heterotrophic respiration rate at 0 $^{\circ}\text{C}$	$\text{g g}^{-1} \text{ month}^{-1}$	[0.0005, 0.007]
<i>KFALL</i>	Proportion of vegetation carbon loss as litterfall monthly	$\text{g g}^{-1} \text{ month}^{-1}$	[0.0005, 0.005]
N_{max}	Maximum rate of N uptake by vegetation	$\text{g m}^{-2} \text{ month}^{-1}$	[0.1, 1.0]
N_{up}	Ratio between N immobilized and C respired by heterotrophs	g g^{-1}	[0, 0.05]
<i>NFALL</i>	Proportion of vegetation nitrogen loss as litter-fall monthly	$\text{g g}^{-1} \text{ month}^{-1}$	[0.001, 0.01]

904

905

906 Table 4. Statistical results for the observed and SAT-TEM and TEM predicted monthly GPP and NEP at
 907 each AmeriFlux site for parameterization. The units of RMSE are $\text{g C m}^{-2} \text{ month}^{-1}$.
 908

<i>Site Name</i>	<i>Time Periods</i>		R^2	<i>RMSE</i>
Howland Forest West Tower (ME, USA)	2002-2004	<i>SAT-TEM GPP</i>	0.94	27.24
		<i>SAT-TEM NEP</i>	0.65	26.84
		<i>TEM GPP</i>	0.85	64.68
		<i>TEM NEP</i>	0.67	29.72
Harvard Forest (MA, USA)	2002-2006	<i>SAT-TEM GPP</i>	0.90	45.62
		<i>SAT-TEM NEP</i>	0.83	40.84
		<i>TEM GPP</i>	0.87	58.63
		<i>TEM NEP</i>	0.75	64.87
Vaira Ranch (CA, USA)	2004-2007	<i>SAT-TEM GPP</i>	0.90	48.37
		<i>SAT-TEM NEP</i>	0.66	26.40
		<i>TEM GPP</i>	0.23	84.13
		<i>TEM NEP</i>	0.04	44.20
Sky Oaks New (CA, USA)	2006	<i>SAT-TEM GPP</i>	0.10	19.15
		<i>SAT-TEM NEP</i>	0.13	19.03
		<i>TEM GPP</i>	0.30	15.99
		<i>TEM NEP</i>	0.01	34.21
Tonzi Ranch (CA, USA)	2004-2007	<i>SAT-TEM GPP</i>	0.74	32.81
		<i>SAT-TEM NEP</i>	0.52	26.73
		<i>TEM GPP</i>	0.20	66.61
		<i>TEM NEP</i>	0.03	46.76
Bondville (IL, USA)	2003-2006	<i>SAT-TEM GPP</i>	0.87	63.90
		<i>SAT-TEM NEP</i>	0.66	66.20
		<i>TEM GPP</i>	0.50	155.33
		<i>TEM NEP</i>	0.14	103.80

909

910

911 Table 5. Statistics for the observed and SAT-TEM and TEM predicted monthly GPP and NEP at each
 912 AmeriFlux site for parameterization. The units of RMSE are $\text{g C m}^{-2} \text{ month}^{-1}$.

<i>Site Name</i>	<i>Time Periods</i>		R^2	<i>RMSE</i>
Niwot Ridge (CO, USA)	2000-2005	<i>SAT-TEM GPP</i>	0.90	19.56
		<i>SAT-TEM NEP</i>	0.78	13.64
		<i>TEM GPP</i>	0.83	28.10
		<i>TEM NEP</i>	0.83	12.02
Wind River Crane site (WA, USA)	2000-2002	<i>SAT-TEM GPP</i>	0.83	32.71
		<i>SAT-TEM NEP</i>	0.33	34.29
		<i>TEM GPP</i>	0.74	65.30
		<i>TEM NEP</i>	0.09	42.06
Morgan Monroe State Forest (IN, USA)	2001-2006	<i>SAT-TEM GPP</i>	0.95	41.89
		<i>SAT-TEM NEP</i>	0.91	38.21
		<i>TEM GPP</i>	0.88	54.13
		<i>TEM NEP</i>	0.72	59.84
Willow Creek (WI, USA)	2000-2003	<i>SAT-TEM GPP</i>	0.96	35.15
		<i>SAT-TEM NEP</i>	0.83	38.62
		<i>TEM GPP</i>	0.71	55.38
		<i>TEM NEP</i>	0.73	57.70
Kendall Grassland (AZ, USA)	2005-2007	<i>SAT-TEM GPP</i>	0.61	37.35
		<i>SAT-TEM NEP</i>	0.39	17.05
		<i>TEM GPP</i>	0.12	166.23
		<i>TEM NEP</i>	0.02	32.60
Walnut River (KS, USA)	2002-2003	<i>SAT-TEM GPP</i>	0.76	57.04
		<i>SAT-TEM NEP</i>	0.58	25.43
		<i>TEM GPP</i>	0.36	75.22
		<i>TEM NEP</i>	0.02	46.99
Sky Oaks Old (CA, USA)	2004-2006	<i>SAT-TEM GPP</i>	0.09	16.42
		<i>SAT-TEM NEP</i>	0.19	14.21
		<i>TEM GPP</i>	0.01	35.57
		<i>TEM NEP</i>	0.01	30.41
Santa Rita Mesquite Savanna (AZ, USA)	2004-2006	<i>SAT-TEM GPP</i>	0.68	24.78
		<i>SAT-TEM NEP</i>	0.12	20.59
		<i>TEM GPP</i>	0.50	21.87
		<i>TEM NEP</i>	0.03	22.78
Rosemount G21 Conventional Management Corn Soybean Rotation (MN, USA)	2004-2006	<i>SAT-TEM GPP</i>	0.69	93.04
		<i>SAT-TEM NEP</i>	0.56	55.58
		<i>TEM GPP</i>	0.51	138.89
		<i>TEM NEP</i>	0.27	73.11
Mead Irrigated Rotation (NE, USA)	2002-2005	<i>SAT-TEM GPP</i>	0.66	128.83
		<i>SAT-TEM NEP</i>	0.29	105.89
		<i>TEM GPP</i>	0.56	180.60
		<i>TEM NEP</i>	0.26	116.52

914 Table 6. Estimated annual GPP, NPP and NEP across conterminous United States over 2000-2005. The
 915 units of the carbon fluxes are Pg C yr⁻¹.

<i>Year</i>	<i>GPP</i>		<i>NPP</i>		<i>NEP</i>	
	<i>SAT-TEM</i>	<i>TEM</i>	<i>SAT-TEM</i>	<i>TEM</i>	<i>SAT-TEM</i>	<i>TEM</i>
2000	7.24±0.33	8.85	3.85±0.63	4.87	0.33±0.18	-0.31
2001	7.35±0.35	9.32	4.06±0.63	5.27	0.41±0.17	0.02
2002	7.02±0.34	9.38	3.81±0.62	5.32	0.08±0.17	0.18
2003	7.44±0.35	10.11	4.12±0.65	5.86	0.40±0.17	0.70
2004	7.75±0.34	8.96	4.38±0.65	4.96	0.73±0.18	-0.19
2005	7.78±0.35	10.35	4.20±0.69	6.04	0.53±0.18	0.69
Average	7.43±0.34	9.49	4.07±0.65	5.39	0.41±0.18	0.18

916

917

918 Table 7. Comparison of carbon fluxes between TEM estimated and other existing estimates in the conterminous United States

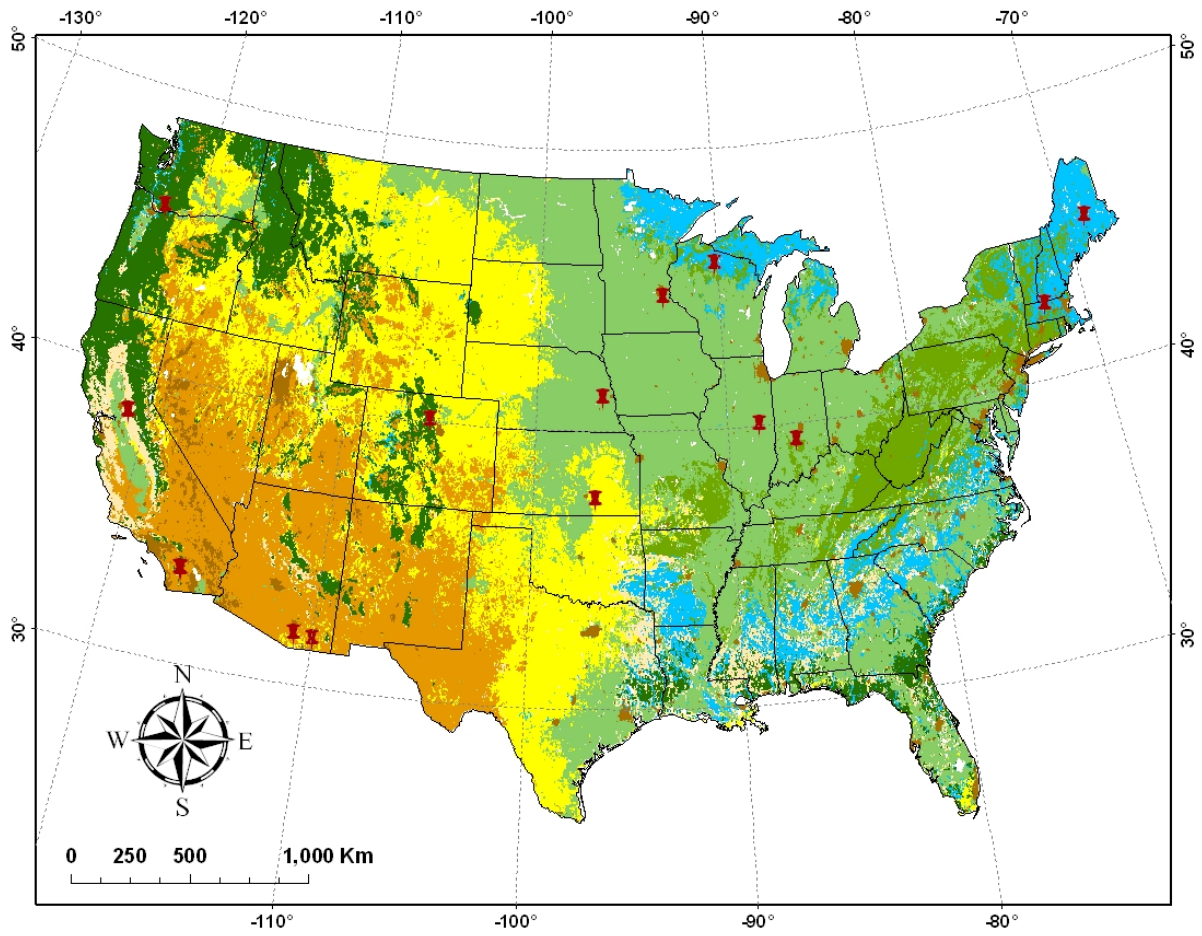
Method	Reference	Time Period	Estimated averaged annual GPP (Pg C yr ⁻¹)	Estimated averaged annual NPP (Pg C yr ⁻¹)	Estimated averaged annual NEP (Pg C yr ⁻¹)	Comments
SAT-TEM						
<i>Ecosystem Model combining satellite observations</i>		2000-2005	7.43	4.07	0.41	Estimated in this study.
TEM	(McGuire et al., 1992; Zhuang et al., 2003)	2000-2005	9.49	5.39	0.18	Estimated in this study.
MOD17	(Zhao et al., 2005; Running et al., 2004)	2000-2005	6.2	3.3		Aggregated form MODIS primary production products (MOD17)
NASA-CASA	(Potter et al., 2007; Potter et al., 1993)	2000-2004		2.65	0.13	
EC-MOD	(Xiao et al., 2010; Xiao et al., in press)	2001-2006	7.06		1.21	The author presented 0.63 Pg C yr ⁻¹ as the total carbon sink for considering the carbon assimilated by crops would be released back to atmosphere. We added the cropland contribution 0.58 Pg C yr ⁻¹ here to be consistent with our study region.
Nested inverse modeling	(Deng et al., 2007)	2003			0.63	Calculated by subtracting Canada sink from the North America total sink

919 Table 8. TEM estimated annual carbon fluxes for each vegetation type in the conterminous United
 920 States during 2000-2005.

<i>Vegetation Type</i>	<i>Total Annual GPP (PgC yr⁻¹)</i>	<i>Total Annual NPP (PgC yr⁻¹)</i>	<i>Total Annual NEP (PgC yr⁻¹)</i>	<i>Mean Annual GPP (kgCm⁻²yr⁻¹)</i>	<i>Mean Annual NPP (kgCm⁻²yr⁻¹)</i>	<i>Mean Annual NEP (kgCm⁻²yr⁻¹)</i>	<i>Land Area (km²)</i>
<i>Evergreen Forest</i>	1.50	0.57	0.038	1.46	0.55	0.037	1,028,790
<i>Deciduous Forest</i>	1.28	0.95	0.110	1.53	1.13	0.131	838,203
<i>Grassland</i>	1.31	0.83	0.075	0.75	0.48	0.043	1,745,960
<i>Shrubland</i>	0.25	0.08	0.015	0.18	0.06	0.011	1,355,240
<i>Savannas</i>	0.39	0.27	0.012	1.34	0.93	0.041	290,155
<i>Cropland</i>	2.85	1.45	0.178	1.25	0.63	0.078	2,287,000

921

922 Figure 1.



923

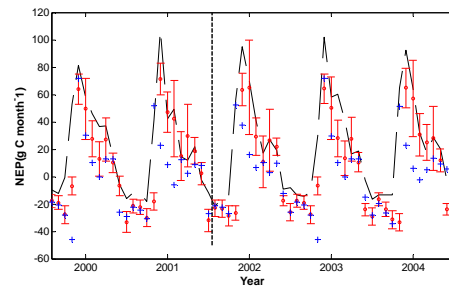
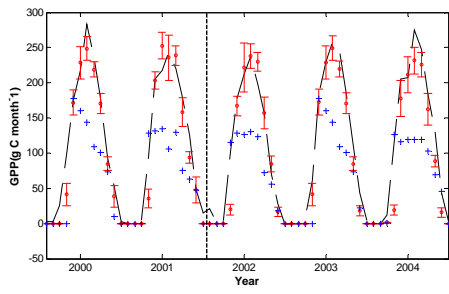
‡ AmeriFlux Sites

- Urban & Barren** **Mixed Forest** **Evergreen Forest** **Deciduous Forest**
- Grassland** **Shrubland** **Savanna** **Cropland**

924

925

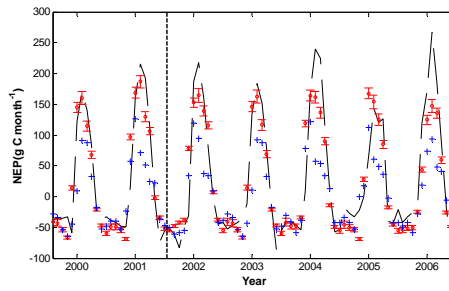
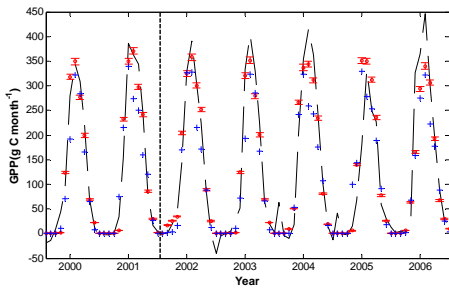
926 Figure 2.



927

928

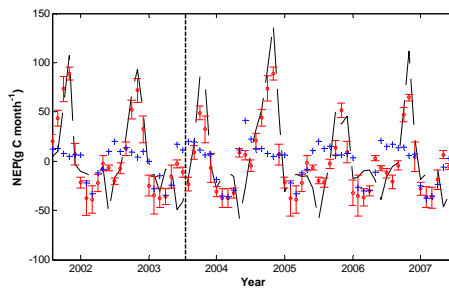
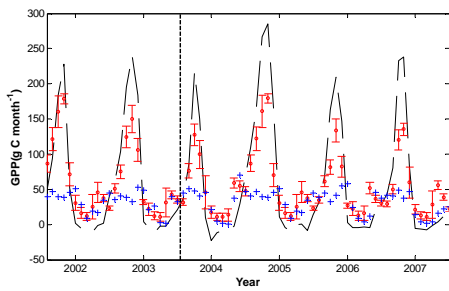
(a)



929

930

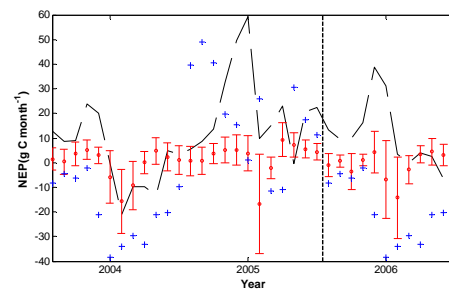
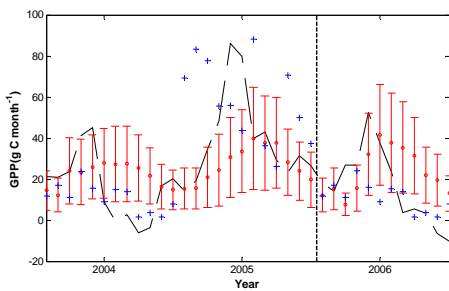
(b)



931

932

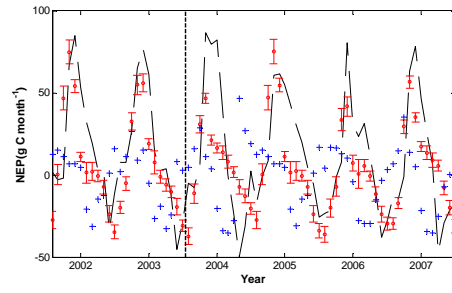
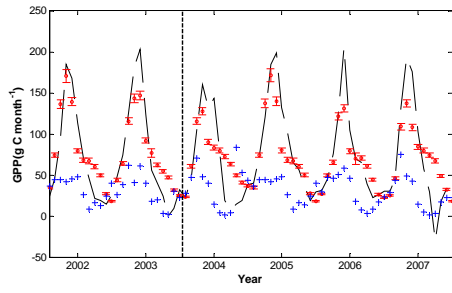
(c)



933

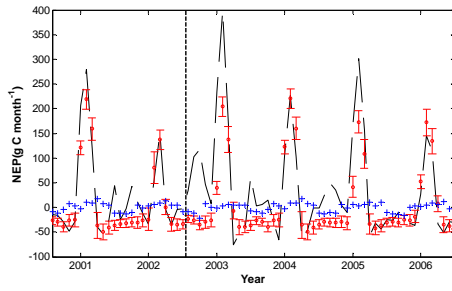
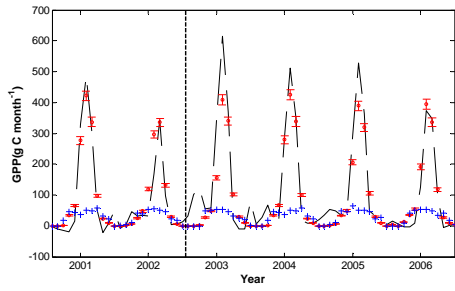
934

(d)



935
936

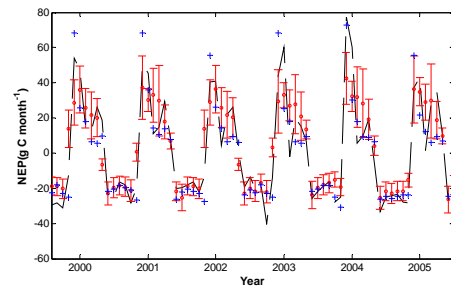
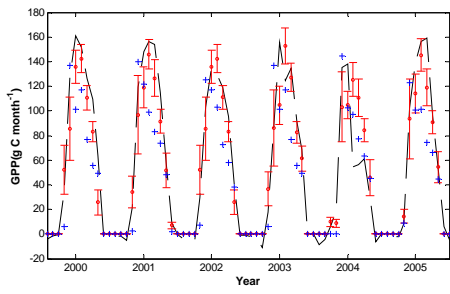
(e)



937
938
939

(f)

940 Figure 3.

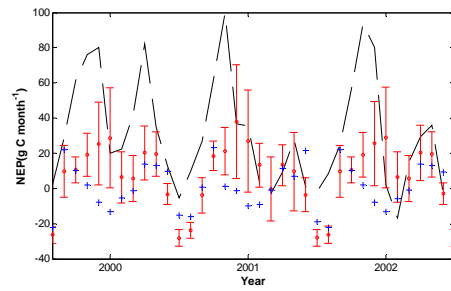
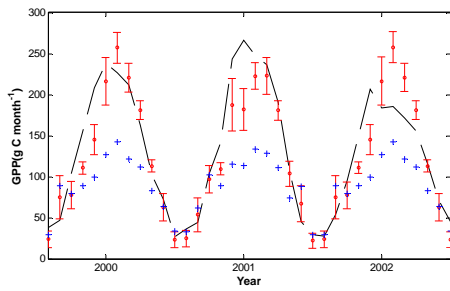


941

942

943

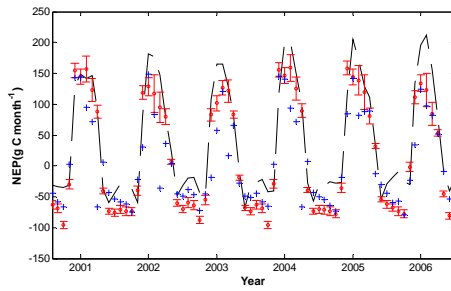
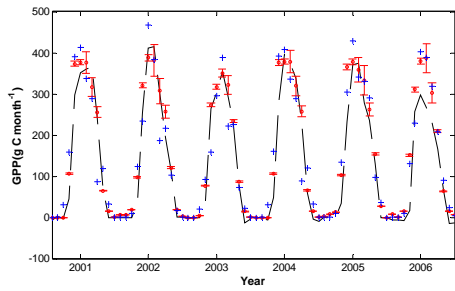
(a)



944

945

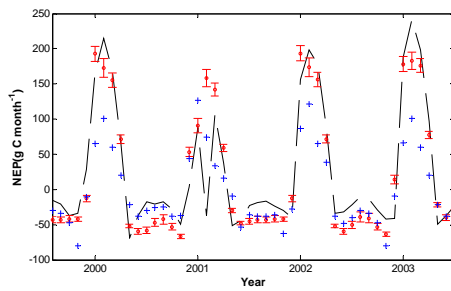
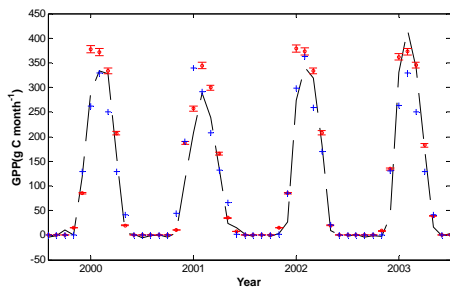
(b)



946

947

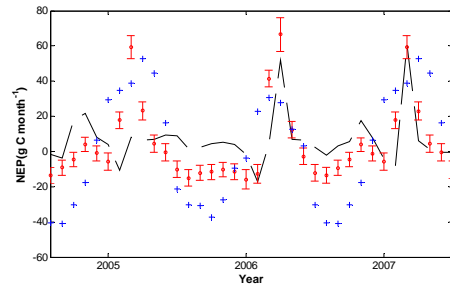
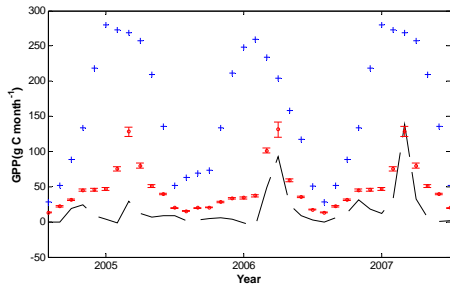
(c)



948

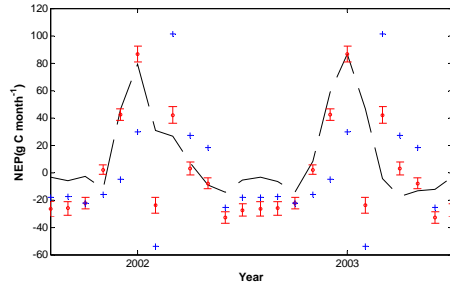
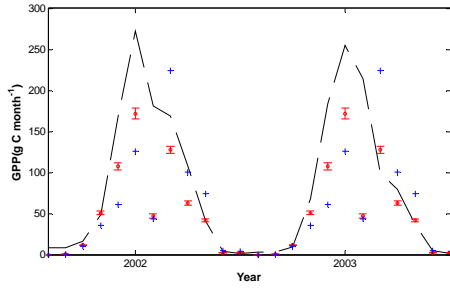
949

(d)



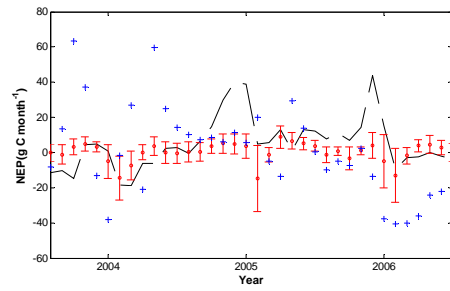
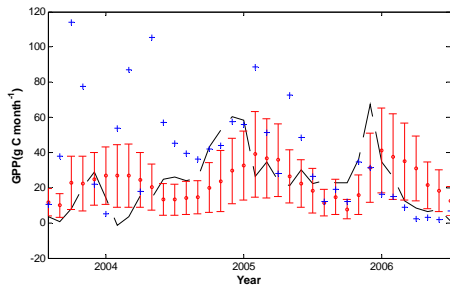
950
951

(e)



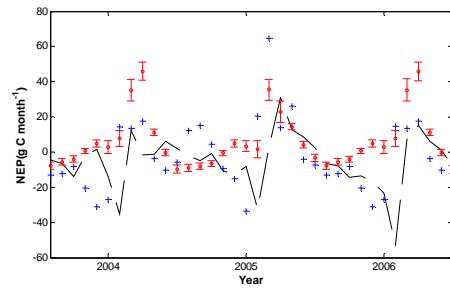
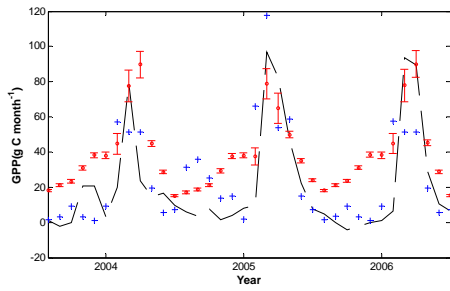
952
953

(f)



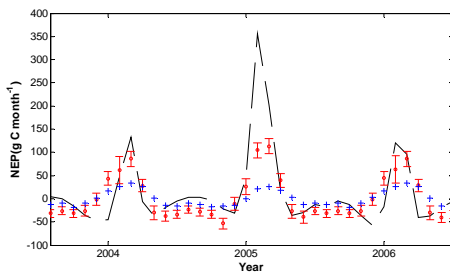
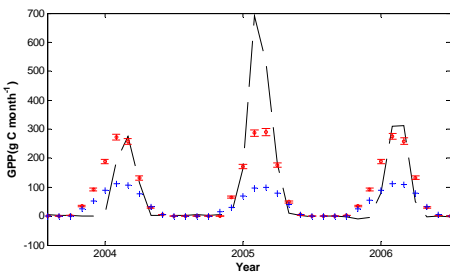
954
955

(g)



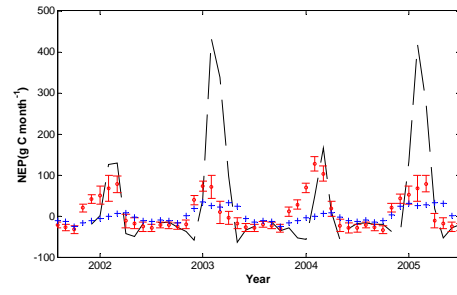
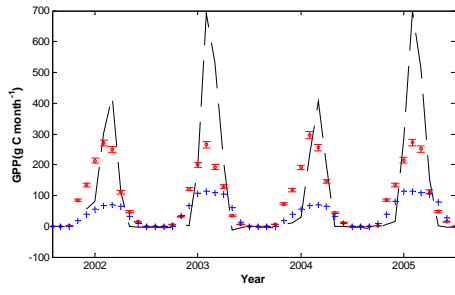
956
957

(h)



958
959

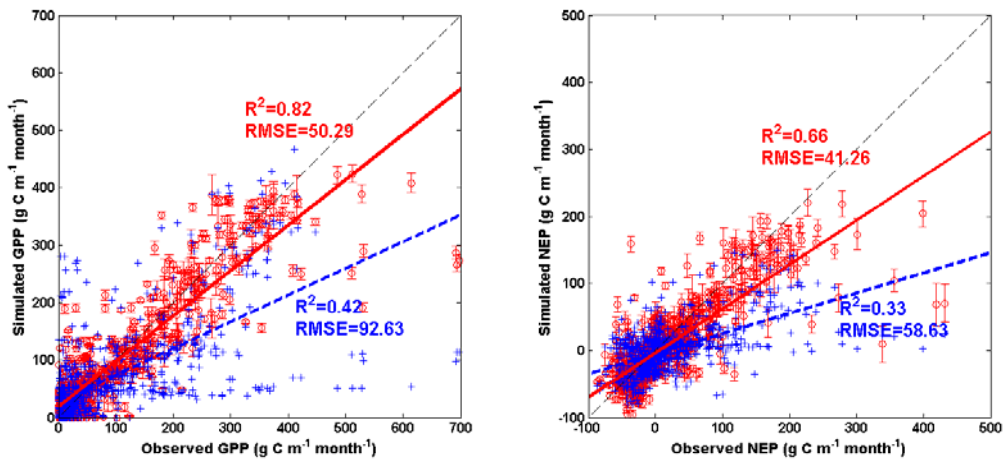
(i)



960
961
962
963
964

(j)

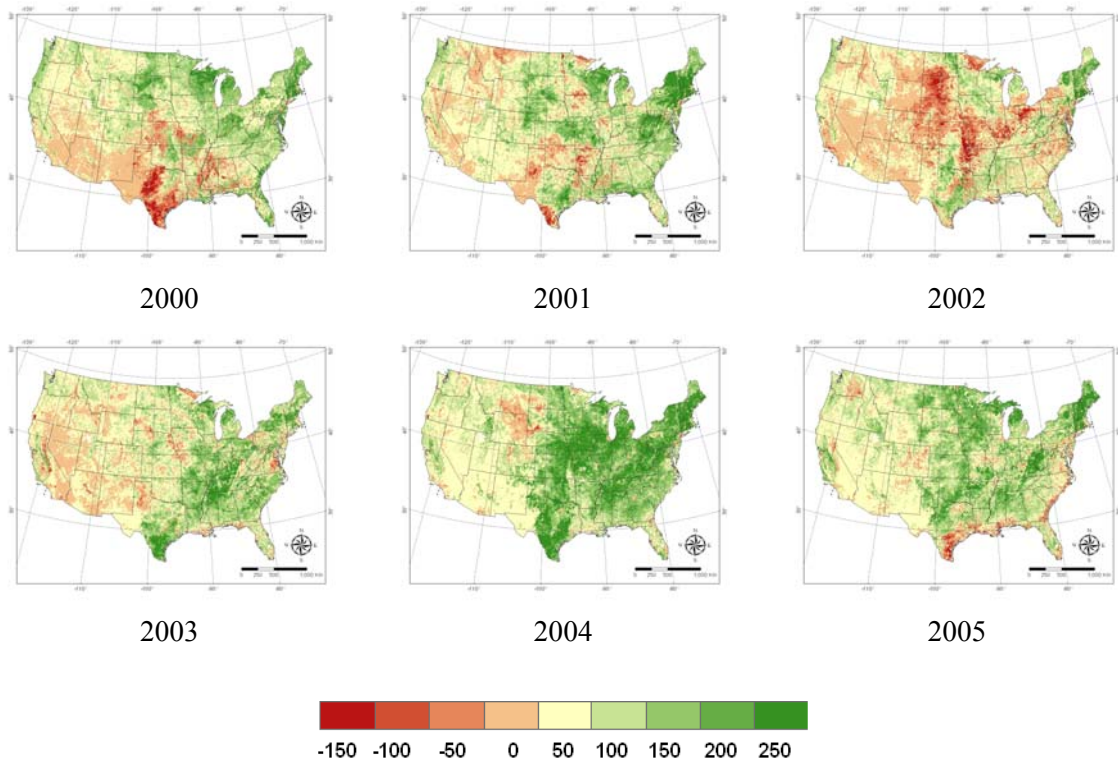
965 Figure 4.



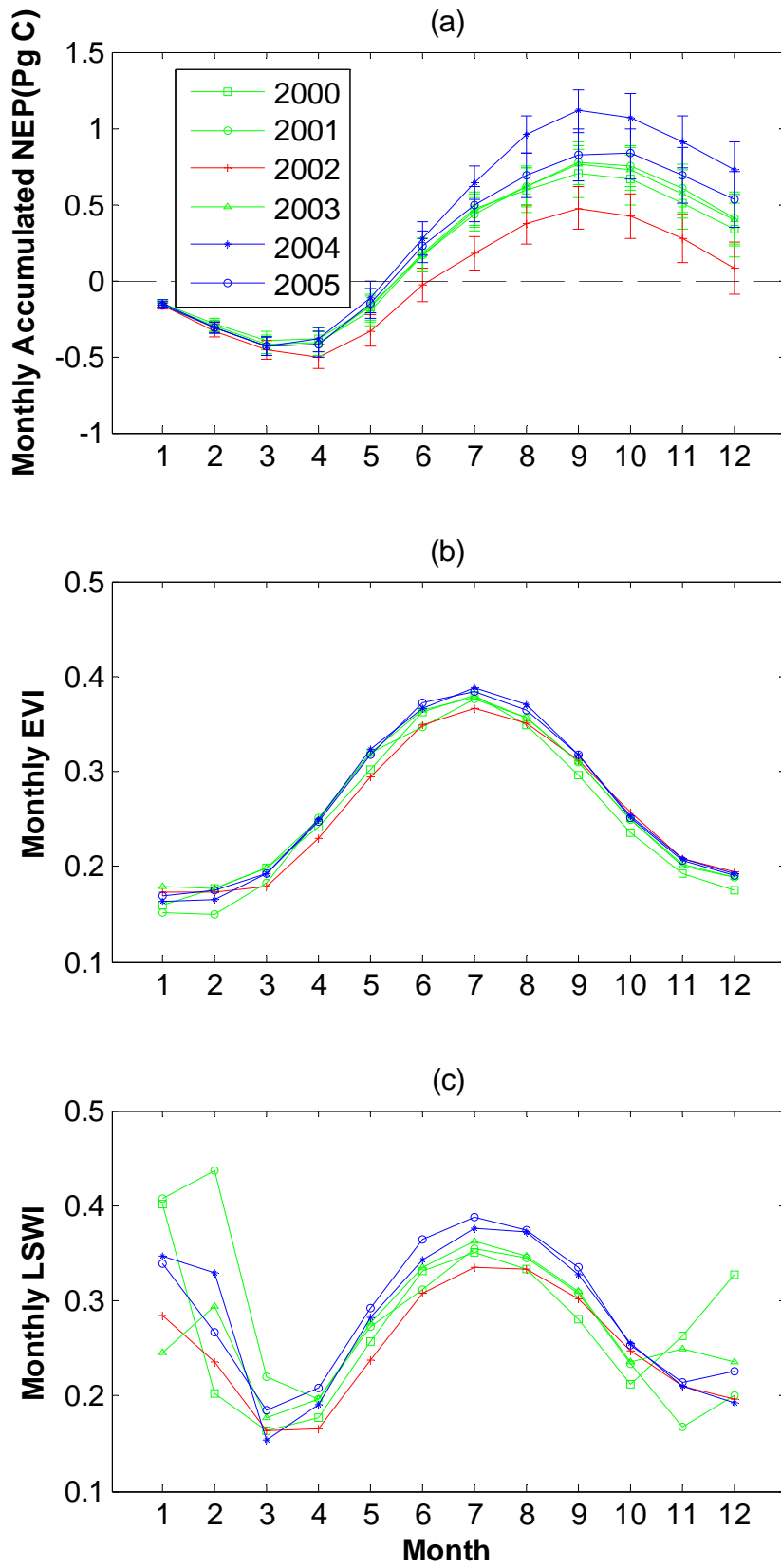
966

967

968 Figure 5.

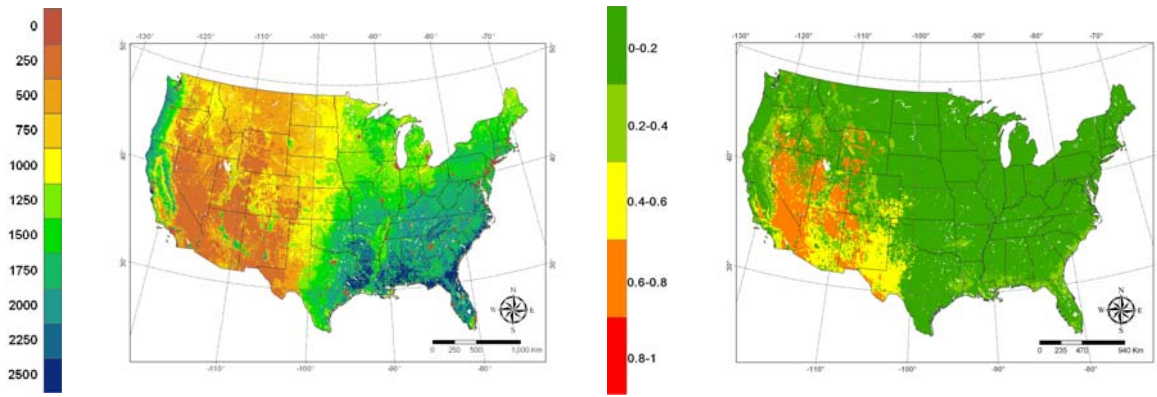


969

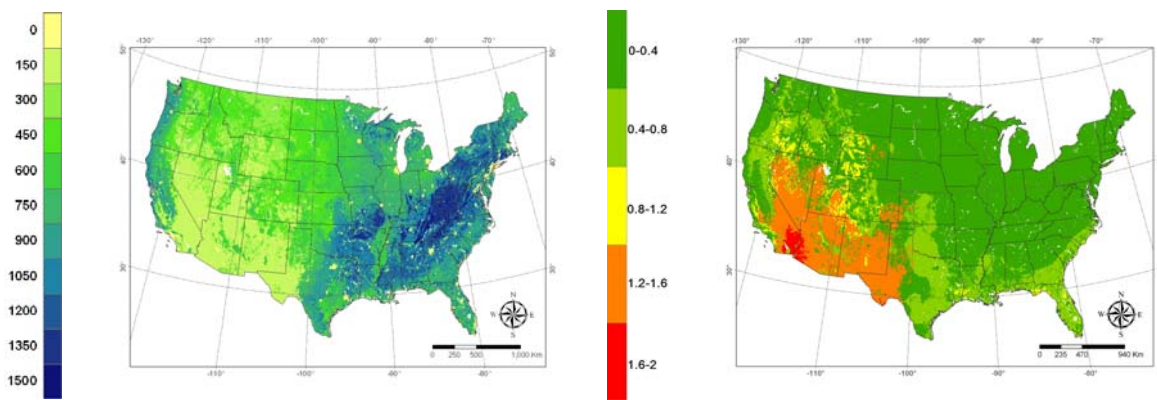


971
972
973

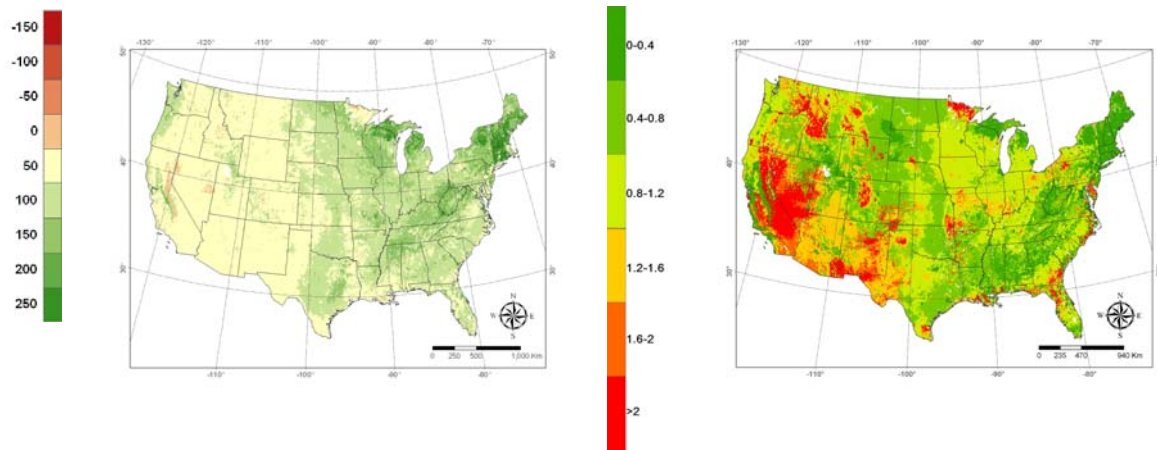
974 Figure 7.



(a) GPP



(b) NPP

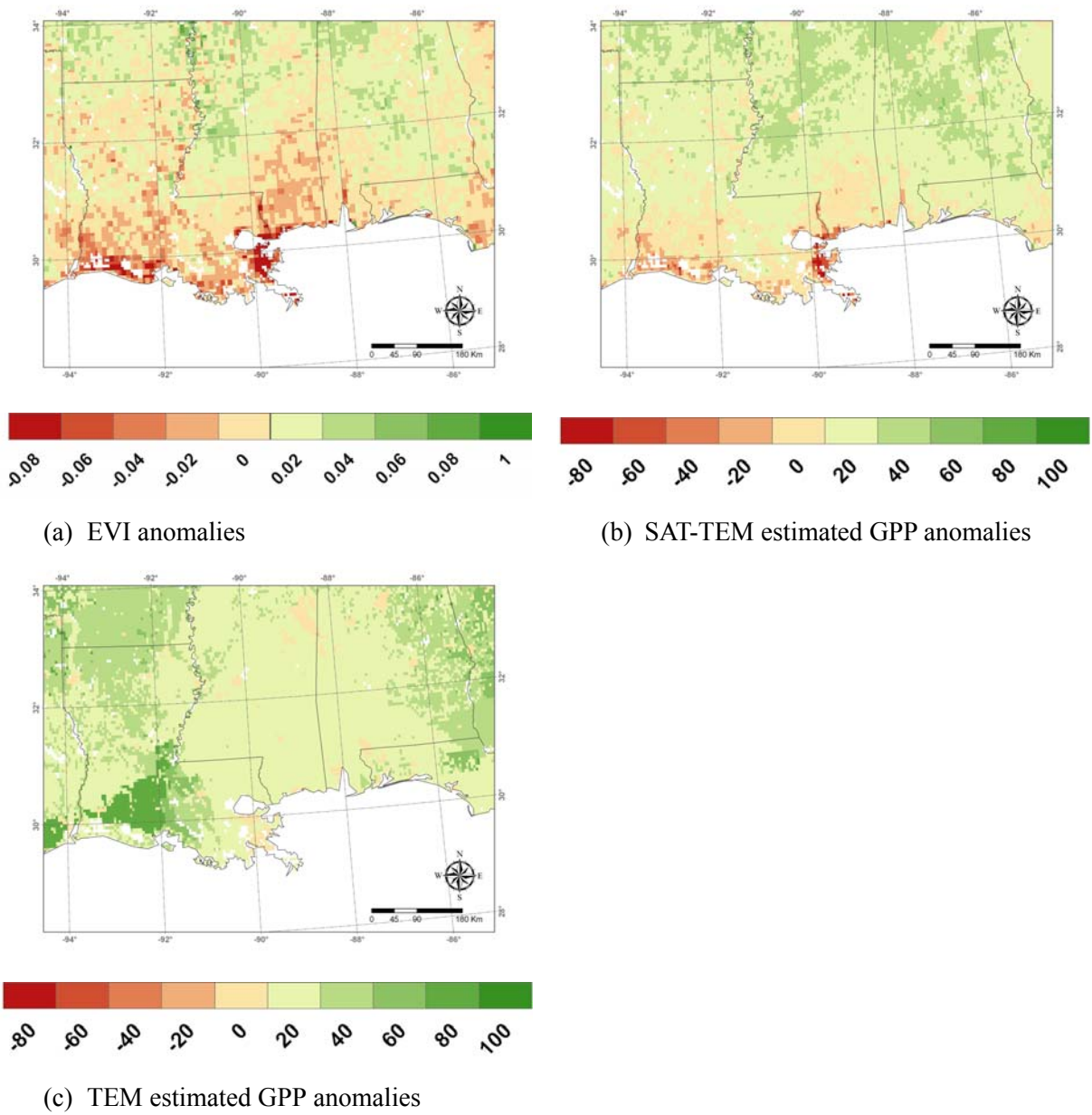


(c) NEP

975

976

977 Figure 8.



978